Quaternary Science Reviews 30 (2011) 1047–1066

Contents lists available at ScienceDirect

Quaternary Science Reviews

journal homepage: www.elsevier.com/locate/quascirev

A new concept for the paleoceanographic evolution of Heinrich event 1 in the North Atlantic

J.D. Stanford [a,*], E.J. Rohling [a], S. Bacon [a], A.P. Roberts [a,b], F.E. Grousset [c], M. Bolshaw [a]

[a] School of Ocean and Earth Science, National Oceanography Centre, University of Southampton, Southampton SO14 3ZH, United Kingdom
[b] Research School of Earth Sciences, ANU College of Physical and Mathematical Sciences, The Australian National University, Canberra 0200, Australia
[c] Département de Géologie et Océanographie, UMR 5805 EPOC, Université Bordeaux 1, Talence, France

ARTICLE INFO

Article history:
Received 26 January 2010
Received in revised form
1 February 2011
Accepted 7 February 2011
Available online 22 April 2011

Keywords:
Heinrich event 1
North Atlantic deep water formation
Nordic seas

ABSTRACT

New records of planktonic foraminiferal $\delta^{18}O$ and lithic and foraminiferal counts from Eirik Drift are combined with published data from the Nordic Seas and the "Ice Rafted Debris (IRD) belt", to portray a sequence of events through Heinrich event 1 (H1). These events progressed from an onset of meltwater release at ~19 ka BP, through the 'conventional' H1 IRD deposition phase in the IRD belt starting from ~17.5 ka BP, to a final phase between 16.5 and ~15 ka BP that was characterised by a pooling of freshwater in the Nordic Seas, which we suggest was hyperpycnally injected into that basin. After ~15 ka BP, this freshwater was purged from the Nordic Seas into the North Atlantic, which preconditioned the Nordic Seas for convective deep-water formation. This allowed an abrupt re-start of North Atlantic Deep Water (NADW) formation in the Nordic Seas at the Bølling warming (14.6 ka BP). In contrast to previous estimates for the duration of H1 (i.e., 1000 years to only a century or two), the total, combined composite H1 signal presented here had a duration of over 4000 yrs (~19–14.6 ka BP), which spanned the entire period of NADW collapse. It appears that deep-water formation and climate are not simply controlled by the magnitude or rate of meltwater addition. Instead the location of meltwater injections may be more important, with NADW formation being particularly sensitive to surface freshening in the Arctic/Nordic Seas.

1. Introduction

Heinrich (H) events are characterised in North Atlantic sediments by horizons with increased Ice Rafted Debris (IRD) concentrations, low foraminiferal abundances, and light planktonic foraminiferal calcite $\delta^{18}O$ (meltwater dilution). They occurred quasi-periodically with a spacing of 5000–14,000 yrs (e.g., Heinrich, 1988; Broecker, 1994; Broecker et al., 1992; Bond et al., 1992, 1999; Bard et al., 2000; Rohling et al., 2003; Hemming, 2004), and most likely ~7200 yrs (van Kreveld et al., 2000). These layers are distinct in marine sediment cores recovered from the so-called "IRD belt" (40°N–55°N), but they can also be recognised throughout most of the North Atlantic (e.g., Heinrich, 1988; Broecker, 1994; Broecker et al., 1992; Bond et al., 1992, 1999; Bond and Lotti, 1995; Cortijo et al., 1997; Hemming et al., 2000, 2002; Hemming and Hajdas, 2003; Grousset et al., 1993, 2000, 2001; for a review, see Hemming, 2004). IRD can even be found as far south as the subtropical gyre; for example, the north Sargasso Sea (Keigwin and Boyle, 1999; Benetti, 2006; Gil et al., 2009) and the Iberian margin (Bard et al., 2000).

It is thought that H events mainly represent periodic collapses of the Laurentide ice sheet (MacAyeal, 1993), although there are strong indications that the Greenland, Icelandic, Fennoscandian, and British ice sheets were also involved (e.g., Bond et al., 1997, 1999; Scourse et al., 2000; Knutz et al., 2001, 2007; Grousset et al., 2001; Hemming et al., 2000; Hemming, 2004; Jullien et al., 2006; Nygård et al., 2007; Peck et al., 2006, 2007b). Furthermore, records from around the North Atlantic, and even throughout the Northern Hemisphere, indicate dramatic marine and terrestrial temperature reductions and increased aridity during H events (e.g., Atkinson et al., 1987; Alm, 1993; Bond et al., 1992; Mayewski et al., 1994, 1997; Vidal et al., 1999; Broecker, 2000; Bard et al., 2000; Gasse, 2000; Rohling et al., 2003; Hemming, 2004). The most widely accepted hypothesis holds that the low temperatures associated with these events resulted from reduced oceanic poleward heat transport due to surface freshwater dilution in the North Atlantic and a consequent shutdown of the Atlantic meridional overturning circulation (AMOC) (e.g., Broecker, 1991; Rahmstorf,

* Corresponding author.
E-mail address: jstan@noc.soton.ac.uk (J.D. Stanford).

0277-3791/$ – see front matter © 2011 Elsevier Ltd. All rights reserved.
doi:10.1016/j.quascirev.2011.02.003

1994; Ganopolski et al., 1998; Ganopolski and Rahmstorf, 2001; Rahmstorf, 2002; Kim et al., 2002; Schmittner et al., 2003).

Sediment cores from the IRD belt suggest a common age for H1 (the last major H event occurring at the onset of the deglaciation) between 16 and 17.5 thousand years before present (ka BP, where present refers to AD 1950) (e.g., Bond et al., 1992, 1997, 1999; Bard et al., 2000; Grousset et al., 2001; Rohling et al., 2003; Hemming, 2004; McManus et al., 2004), in which case it had terminated well before the abrupt Bølling warming (14.64 ka BP) (Lea et al., 2003; Rasmussen et al., 2006). Coincident with this timing of H1, $^{231}Pa/^{230}Th$ ratios recorded in a Bermuda Rise sediment core GGC5 suggest virtually complete AMOC shutdown (McManus et al., 2004). However, this proxy for AMOC intensity suggests a gradual slowdown from around 19 ka BP into the AMOC collapse, and a sharp AMOC resumption coincident with the Bølling warming (McManus et al., 2004). The $^{231}Pa/^{230}Th$ method underlying these reconstructions has been challenged (e.g., Keigwin and Boyle, 2008; Gil et al., 2009) but, the GGC5 $^{231}Pa/^{230}Th$ record has been independently corroborated by magnetic grain size data from core TTR13-AT451G (1927 m water depth; 58°30.886'N; 44°54.333'W) (hereafter referred to as TTR-451), recovered from Eirik Drift, offshore of S. Greenland (Stanford et al., 2006). The timing presented by McManus et al. (2004) of the gradual slowdown from around 19 ka BP to full AMOC collapse at around 17.5 ka BP has also been corroborated by a $^{231}Pa/^{230}Th$ record from a drift deposit in the Rockall Trough (Hall et al., 2006). Reduced deep-water ventilation and, hence, decreased AMOC intensity during H1 have also been inferred from $\delta^{13}C$ records, and from deep-water ^{14}C ages and Cd/Ca ratios (e.g., Boyle and Keigwin, 1987; Boyle, 1992; Sarnthein et al., 1994; Curry et al., 1999; van Kreveld et al., 2000; Robinson et al., 2005; Marchitto et al., 2007; Keigwin and Boyle, 2008).

Marine sediment core TTR-451 (Fig. 1) was recovered from Eirik Drift, beneath the modern pathway of the East Greenland Current (EGC), which today constitutes the main mechanism for the export of cold and relatively fresh surface waters out of the Arctic (Aagaard and Carmack, 1989; Bacon et al., 2002; Holliday et al., 2009). Eirik Drift is a contourite formed from deposition of suspended sediment in Proto North Atlantic Deep Water (Proto-NADW) as it rounds the southern tip of Greenland (Chough and Hesse, 1985; Hunter et al., 2007a; b). Sediments from core TTR-451 therefore record changes in the intensity of Proto-NADW flow.

Here, we investigate co-registered records of stable oxygen isotopes from the calcite tests of the planktonic foraminiferal species *Neogloboquadrina pachyderma* (left-coiling), IRD/lithic counts of grains (>150 μm) per gram of dried sediment, numbers of planktonic foraminifera (>150 μm) per gram of dried sediment, and the ratio of susceptibility of anhysteretic remanent magnetization (κ_{ARM}) to low-field magnetic susceptibility (κ) for core TTR-451. This combination of analyses enables investigation into changes in both surface and deep-water currents that exited the Nordic Seas during H1. We combine our results from Eirik Drift with proxy records from around the North Atlantic and Nordic Seas for the time interval that spans H1, from marine sediment cores SU90-09 (43°05'N, 31°05'W, 3375 m water depth), MD95-2010 (66°41'N,

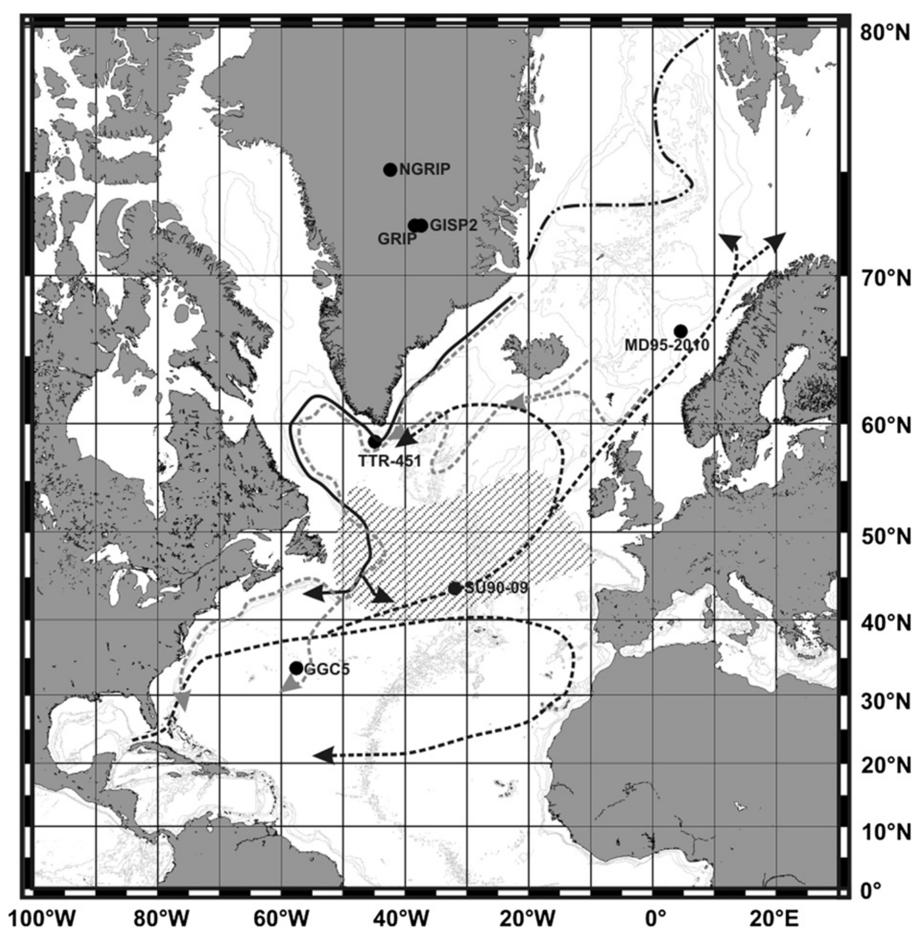

Fig. 1. Map of the North Atlantic with sediment and ice core sites and the likely surface and deep hydrographies for the LGM after Bard et al. (2000) and Pflaumann et al. (2003). The IRD belt (hashed area) is after Hemming (2004). Deep currents are indicated in grey, warm surface currents are indicated with dashed black arrows, and cold surface currents with continuous black arrows. Summer and winter sea-ice margins, after Pflaumann et al. (2003), are shown with a 'dash-dot' line, and a dashed line, respectively.

04°34'E, 1226 m water depth), and GGC5 (33°42'N, 57°35'W, 4550 m water depth). Records from these cores were published previously by Grousset et al. (2001), Dokken and Jansen (1999), and McManus et al. (2004), respectively, and their locations are shown in Fig. 1. We also present a synthesis of the timings of global ice sheet and glacier advances and retreats, and we compare them with sea-level and circum-North Atlantic terrestrial temperature proxy records through the Last Glacial Maximum (LGM), H1 and the Bølling warming. We consider H1 in the wider context rather than just the changes associated with the IRD event, as the transient, process point of view is important in understanding the drivers behind the climate anomalies. These events are then placed in the context of North Atlantic surface and deep-water hydrographic changes. We provide a review on various aspects of the North Atlantic hydrography during H1, and we aim to elucidate the evolution of H1 in the northern North Atlantic, with specific attention to the Nordic Seas, and to reconcile the sequence of events associated with H1 in the North Atlantic to the entire period of AMOC collapse.

2. Methods

κ_{ARM}/κ ratios for core TTR-451 were determined from discrete samples and were cross-validated by comparing additional u-channel κ_{ARM} measurements (not shown) with higher-resolution whole core magnetic susceptibility data (Fig. 2b). The whole core κ was measured with a Bartington Instruments MS2E1 point sensor that was placed in contact with the surface of a split core (labelled as 'whole core' in Fig. 2b). The discrete sample κ measurements were made using a Kappabridge KLY-4 magnetic susceptibility meter, and κ_{ARM} was imparted using a 50 μT bias field and an alternating field of 100 mT, with measurements made using a 2-G Enterprises cryogenic magnetometer in a magnetically shielded laboratory.

Core TTR-451 was sub-sampled continuously at 0.5-cm intervals from a previously collected u-channel sample (2 × 2 cm cross-section). The sediment was prepared by freeze drying, weighing, and wet sieving at 63 μm. It was then oven dried, weighed and dry sieved, and the total weight of the >150 μm sediment fraction was recorded. The sediment was then split into aliquots: one for stable

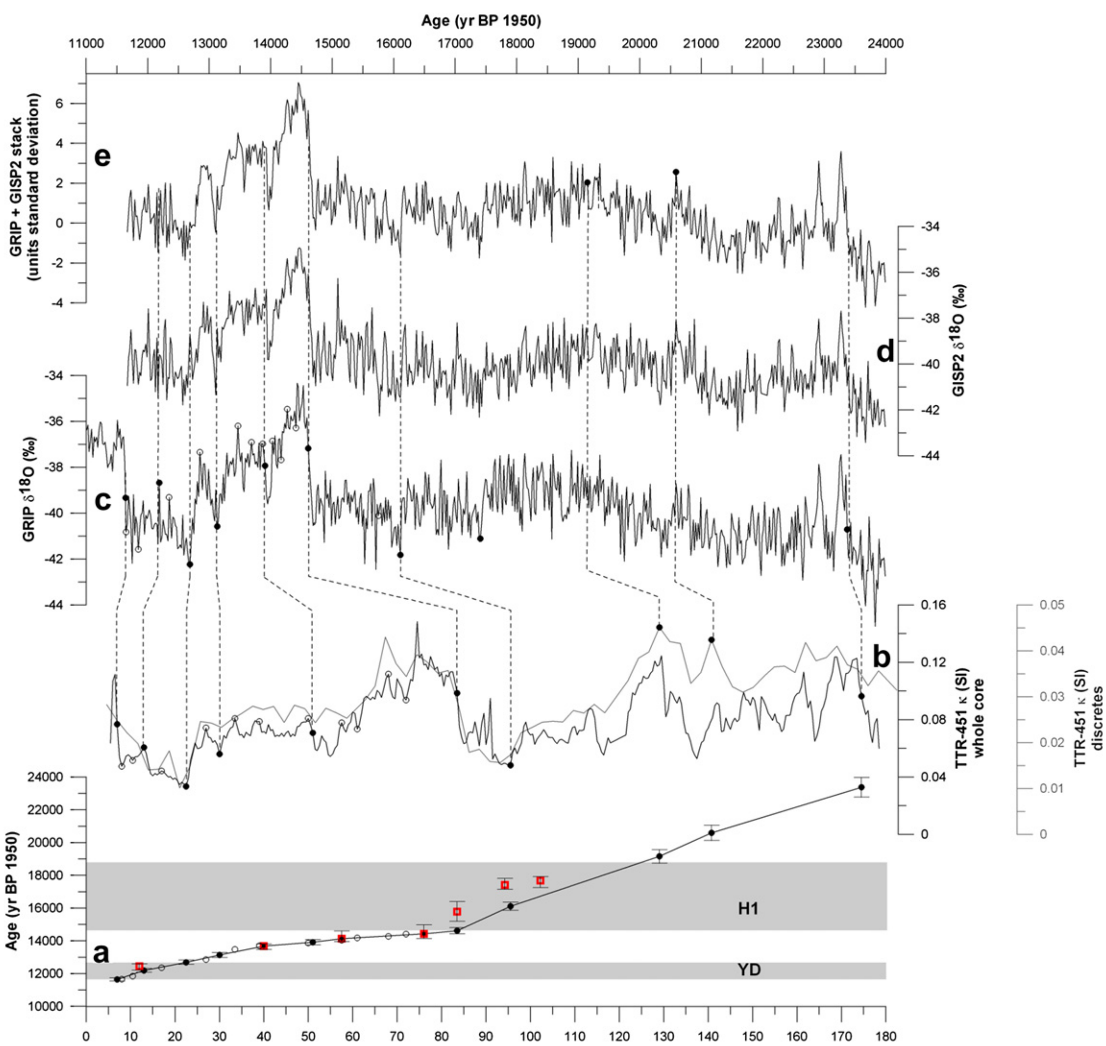

Fig. 2. a. Depth versus age plot for core TTR-451. Open, red squares indicate calibrated AMS^{14}C datings, and error bars indicate 2σ uncertainty ranges (Table 1). Solid black dots indicate tie points from the correlation between magnetic susceptibility and the GRIP ice-core δ^{18}O record; open black circles represent extra correlation points that are not used to construct the age model, but are shown for validation. 2σ error bars indicate the maximum counting error on the GICC05 timescale. Grey areas represent times of reduced NADW ventilation associated with the Younger Dryas and Heinrich Event 1 (McManus et al., 2004). b. Magnetic susceptibility records for TTR-451: black denotes higher-resolution whole core data, and grey denotes lower resolution discrete sample measurements. The GRIP (c) and GISP2 (d) ice core δ^{18}O records are plotted versus the new GICC05 timescale based on layer-counting (Andersen et al., 2006; Svensson et al., 2006; Rasmussen et al., 2006, 2008; Vinther et al., 2006). e. GRIP and GISP2 δ^{18}O records combined to form a regional air-temperature proxy in units standard deviation. YD = Younger Dryas, and H1 = Heinrich event 1.

oxygen isotope analyses and the other for lithic counts. Stable oxygen isotope analyses for core TTR-451 were carried out on 21–32 individuals of *N. pachyderma* (left-coiling) ($\delta^{18}O_{npl}$) with sizes ranging between 225 and 275 μm, using a Europa Geo-2020 mass spectrometer with an individual acid dosing preparation system. Stable isotope ratios are expressed as a 'δ' (delta) value, and are reported as per mil (‰) relative to the Vienna Peedee Belemnite standard (VPDB). External reproducibility as determined using >100 blind standard analyses is better than 0.027‰ for $\delta^{13}C$ and 0.053‰ for $\delta^{18}O$. Lithic counts were performed on the 150 μm fraction of the allocated aliquot using a binocular microscope. On average, ~500 grains were counted per sample, and the grain types were petrologically identified.

3. Results

3.1. Eirik Drift core TTR-451

The chronology of core TTR-451 is primarily constrained by seven accelerator mass spectrometer (AMS) ^{14}C datings of monospecific left-coiling *N. pachyderma* samples that have been calibrated using Calib 6.0.1 (Reimer et al., 2009) with a reservoir age correction $\Delta R = 0$ (Table 1). Within these constraints, the age model is fine-tuned by correlation between the TTR-451 magnetic susceptibility (κ) record and the GRIP ice core stable oxygen isotope ($\delta^{18}O$) record (see correlation lines in Fig. 2). A similar approach has been used in several other studies (e.g., Kissel et al., 1999; Elliot et al., 2002). For further details and discussion, see Stanford et al. (2006). We extend the correlation of TTR-451 and Greenland ice core $\delta^{18}O$ records on the GICC05 timescale (Rasmussen et al., 2006, 2008; Andersen et al., 2006; Svensson et al., 2006) down to the LGM. Low abundances of planktonic foraminifera prior to H1 and a consequent lack of carbonate for AMS ^{14}C dating mean that the age model for this portion of TTR-451 relies entirely upon the correlation shown in Fig. 2. Ice core $\delta^{18}O$ records reflect temperature and air mass variations over the ice sheet (e.g., Dahl-Jensen et al., 1998; Severinghaus et al., 1998; Severinghaus and Brook, 1999; Stuiver and Grootes, 2000). More negative $\delta^{18}O$ generally represent colder conditions, and less negative values represent warmer conditions. The GRIP and GISP2 ice core $\delta^{18}O$ records have significantly different values for the LGM/H1 transition (Fig. 2c, d) despite their close proximity (Fig. 1). Therefore, we consider a mean composite Greenland ice core $\delta^{18}O$ (temperature) record in units standard deviation (Fig. 2e) for the purpose of our correlation.

Stanford et al. (2006) estimated radiocarbon reservoir age correction (ΔR) values using data from core TTR-451. The inferred ΔR for the Younger Dryas ($\Delta R = 351$ yrs, Table 1) compares well (within 1σ) with independently derived ΔR estimates of 371 yrs from cores from the Norwegian margin (Bondevik et al., 2006) and of around 300 yrs by Bard et al. (1994). However, we note that both the AMOC configuration as well as CO_2 transfer may have been very different between H1 and the Younger Dryas. The GICC05 chronology for the GRIP and GISP2 $\delta^{18}O$ records has since been extended beyond 14.7 ka BP (Rasmussen et al., 2006, 2008; Andersen et al., 2006; Svensson et al., 2006). Thus, we provide revised ΔR estimates for H1 (Table 1). A ΔR of 1458 (1912–1081) yrs is inferred for TTR-451 (sample KIA-27859). These ΔR estimates are slightly lower than the ~2000 yrs suggested by Waelbroeck et al. (2001), suggesting that there likely was considerable spatial variability in ΔR during H1.

The sediment accumulation rate in core TTR-451 is found to have been considerably reduced during H1 (Fig. 3a). Relative changes in the abundances of IRD and planktonic foraminifera might have been caused by changes in sediment dilution, so we convert these records for TTR-451 from grains per gram of dried sediment into fluxes (number of grains per cm^2 per year), based on mass accumulation rate (Fig. 3b, c), to permit comparison with other cores (notably SU90-09).

A κ_{ARM}/κ record for core TTR-451 (Stanford et al., 2006) is plotted alongside the $^{231}Pa/^{230}Th$ record for core GGC5 from the Bermuda Rise (McManus et al., 2004) in Fig. 4g. The record of κ_{ARM}/κ (black line in Fig. 4g) gradually increases from ~19 ka BP (note the inverted axis), indicating a slowdown of AMOC intensity, and culminating in a collapse at 17.5 ka BP. A sharp decrease in values at ~14.6 ka BP suggests an abrupt AMOC resumption at the Bølling warming (Fig. 4a, g).

From ~16.7 ka BP a strong shift to lighter $\delta^{18}O_{npl}$ with magnitude of −1.45‰ develops in core TTR-451 (Fig. 4e), which indicates increased freshening that culminates in a broad peak at ~15.1 ka BP. The IRD flux for TTR-451 (Fig. 4d) does not notably increase during this time interval. Planktonic foraminiferal accumulation flux in TTR-451 (Fig. 4c) is generally low during the H1 interval, with a notable minimum between 17.2 and 16.5 ka BP. After the Bølling warm transition at ~14.6 ka BP, $\delta^{18}O_{npl}$ increased to a maximum at ~13.2 ka, followed by decreasing $\delta^{18}O$ into the YD cold period (Fig. 4e). Lithic and planktonic foraminiferal fluxes dramatically increase at ~14.6 ka BP (Fig. 4c, d) and remain variable until the top of core TTR-451 (at about the termination of the Younger Dryas).

3.2. Re-evaluation of terrestrial records of ice sheet and glacier extent and temperature for the LGM, H1 and Bølling warming

We used Calib6.01 (Reimer et al., 2009) to re-calibrate AMS ^{14}C radiocarbon convention ages for terrestrial temperature proxy records (Atkinson et al., 1987; Alm, 1993), terminal moraines, and for marine sediment horizons (Giraudi and Frezzotti, 1997; Benson et al., 1998; McCabe and Clark, 1998; Bowen et al., 2002; Dyke et al., 2002; Marks, 2002; Ivy-Ochs et al., 2006). These re-calibrated datings are used along with previously published calendar ages (e.g., McCabe et al., 2005, 2007) and ^{36}Cl boulder exposure ages (e.g., Bowen et al., 2002; Dyke et al., 2002; Licciardi et al., 2004; Rinterknecht et al., 2006). Results are presented in Fig. 5f and are compared with global sea-level history (Fig. 5d, e), climate

Table 1
AMS ^{14}C measurements and their calibrated (calendar) ages for core TTR-451.

KIA sample number	Depth (cm)	Species	Radiocarbon conventional age	Calibrated age (Calib 6.0.1.)	2σ age range Yrs BP	Inferred ΔR (Yrs)	2σ ΔR range (Yrs)
KIA-26998	12.00	*N. pachy.* (lc)	10905 ± 60 BP	12450 BP	12597–12208 (1)	351	537–85
KIA-27856	40.00	*N. pachy.* (lc)	12220 ± 55 BP	13680 BP	13810–13463 (1)		
KIA-25853	57.50	*N. pachy.* (lc)	12690 ± 55 BP	14130 BP	14593–13938 (0.95) 14866–14712 (0.05)		
KIA-27857	76.00	*N. pachy.* (lc)	12825 ± 55 BP	14422 BP	14974–14126 (1)		
KIA-27858	83.50	*N. pachy.* (lc)	13460 ± 55 BP	15774 BP	16389–15190 (1)	1164	1806–551
KIA-27859	94.25	*N. pachy.* (lc)	14750 ± 60 BP	17418 BP	17805–17125 (1)	1458	1912–1081
KIA-25854	102.25	*N. pachy.* (lc)	14890 ± 60 BP	17672 BP	17907–17239 (1)	972	1338–457

Inferred ΔR values are for AMS ^{14}C datings for the Younger Dryas and Heinrich event 1. KIA = Kiel Institut für Altersbestimmungen. For the calibrated 2σ age ranges, the probabilities for those distributions of ages are given in the brackets.

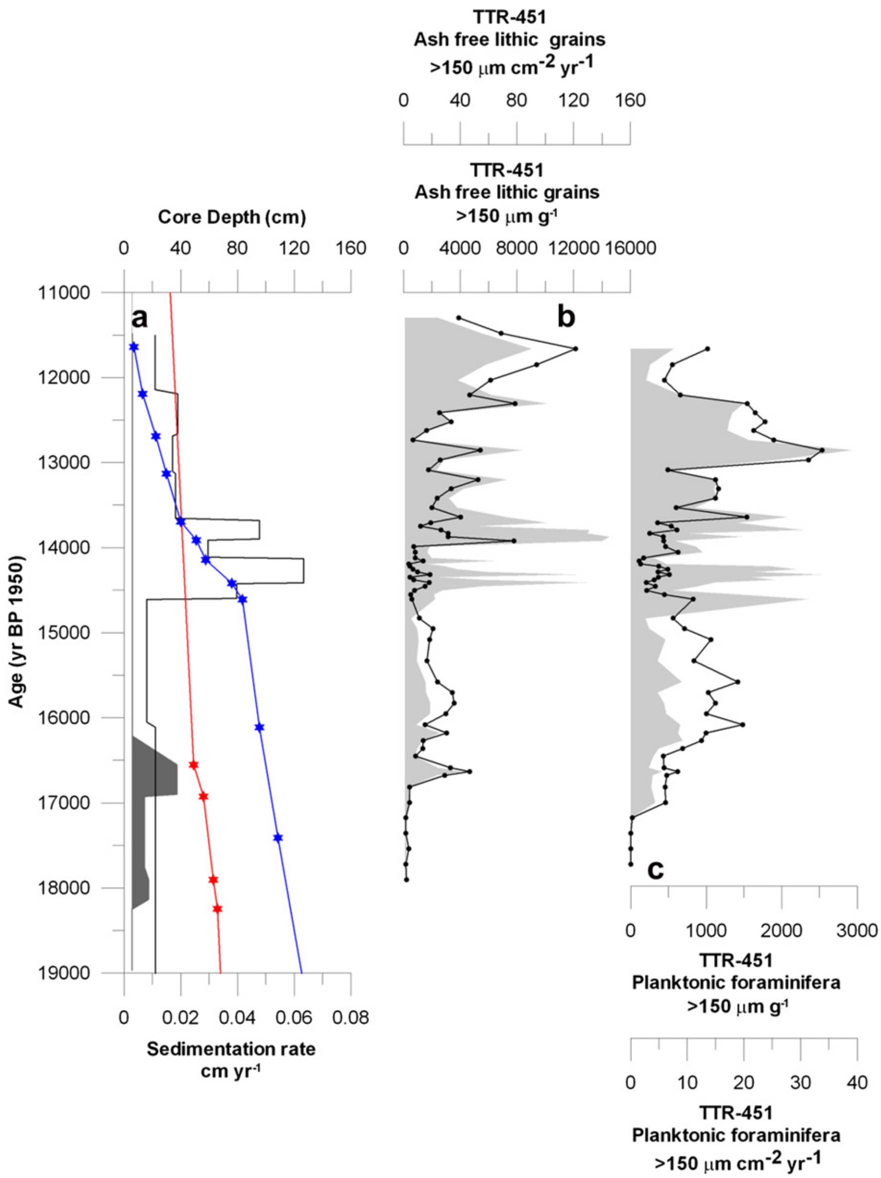

Fig. 3. a. Sedimentation rates for cores TTR-451 (black line) and SU90-09 (grey shading). Age model plots are shown using blue stars for TTR-451 and red stars for SU90-09. b. Number of 'ash' free lithic grains per gram of dried sediment (black line) and the number of 'ash' free lithic grains per cm^2 per year (grey shading) for core TTR-451. *We consider the 'ash' free lithic grains as rhyolite free only, because the morphology of basaltic grains indicates an ice-rafted source. c. The number of planktonic foraminifera per gram of dried sediment (black line) and the number of planktonic foraminifera per cm^2 per year (grey shading.).

variability in Greenland and Antarctica (Fig. 5a–c), and changes in Northern Hemisphere summer insolation (Fig. 5a). Our recalibration of earlier AMS ^{14}C dates for terrestrial records reveals surprising results and our findings are summarised in Table 2. Note, however, that although it is tempting to reconstruct phase relationships from Fig. 5f, this is not warranted because dating uncertainties on boulder exposure ages can exceed 1000 yrs, and because of large differences in the spatial distribution of regional datasets.

4. Discussion

4.1. TTR-451 κ_{ARM}/κ

Our κ_{ARM}/κ record for core TTR-451 (Stanford et al., 2006), and the $^{231}Pa/^{230}Th$ record for core GGC5 from the Bermuda Rise (McManus et al., 2004) (Fig. 4g) offer independent proxies for NADW flow intensity. The chronologies of both records are independent of each other (McManus et al., 2004; Stanford et al., 2006), and both records indicate an AMOC collapse initiating at ~18.8 ka BP, also in agreement with Hall et al. (2006), and an abrupt AMOC resumption at the Bølling warming at ~14.6 ka BP (Fig. 4a, g). The AMOC resumption in both records does not coincide with the 'conventional' termination of H1 (as recorded in sediments from the IRD belt) at ~16 ka BP (e.g., Grousset et al., 2001; Hemming, 2004; Fig. 4e). Instead, it is coincident with the Bølling warming (McManus et al., 2004; Stanford et al., 2006; Fig. 4a, g). This timing for the AMOC flow intensity increase at ~14.6 ka BP underlines suggestions that the AMOC "switch on" and the Bølling warming were intrinsically linked (McManus et al., 2004; Stanford et al., 2006).

4.2. Comparison of H1 records from Eirik Drift with the IRD belt and Nordic Seas

Numbers of planktonic foraminifera and lithic grains >150 μm, and $\delta^{18}O_{npl}$ are shown in Fig. 4c–e, respectively, for core SU90-09 from the central IRD belt (Grousset et al., 2001). Consonant with

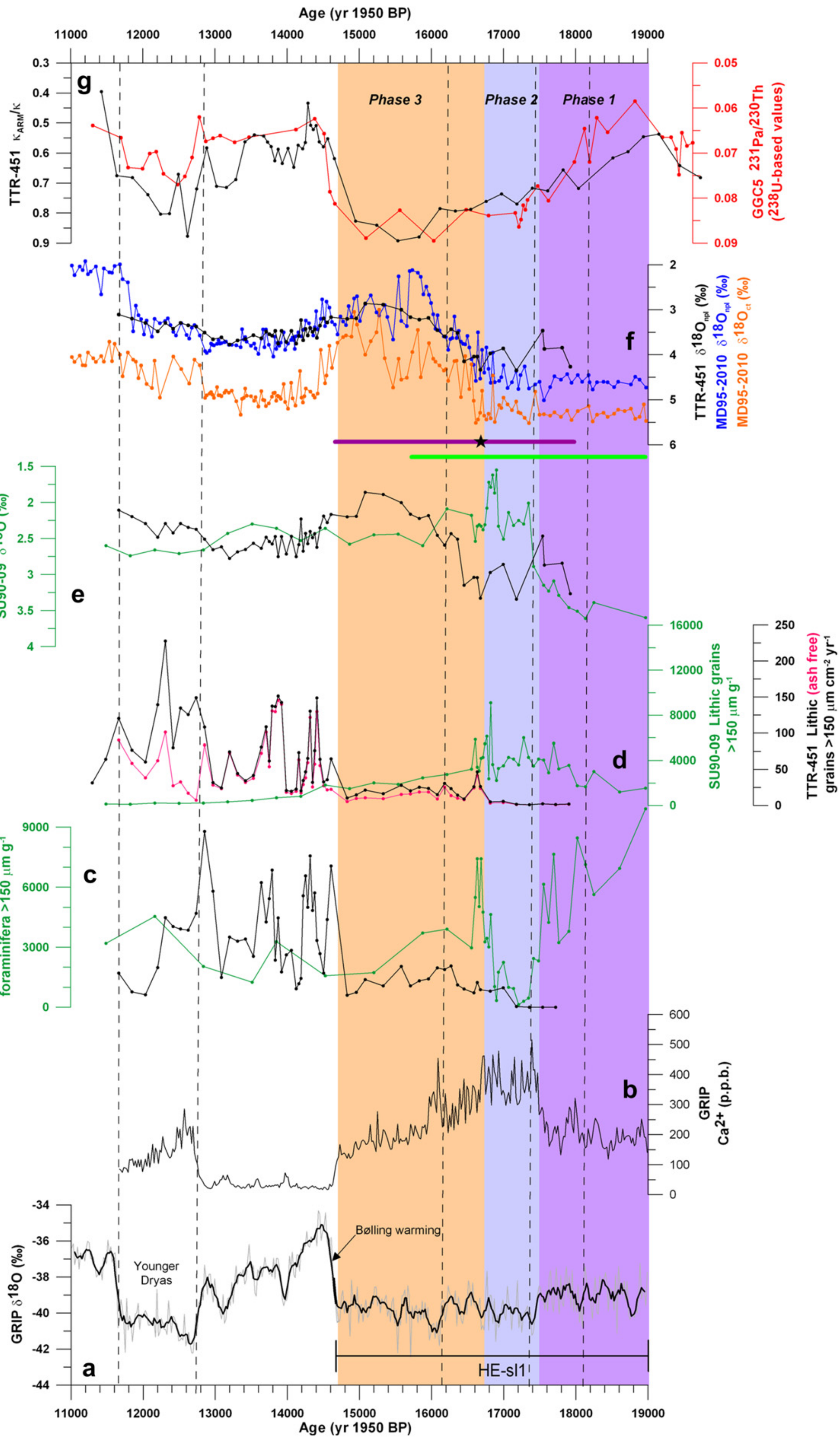

Age (yr 1950 BP)
g
Phase 3
Phase 2
Phase 1
TTR-451 κARM/κ
GGC5 231Pa/230Th (238U-based values)
f
TTR-451 δ18Onpl (‰)
MD95-2010 δ18Onpl (‰)
MD95-2010 δ18Oct (‰)
e
TTR-451 δ18O (‰)
SU90-09 δ18O (‰)
d
SU90-09 Lithic grains >150 μm g-1
TTR-451 Lithic (ash free) grains >150 μm cm-2 yr-1
c
TTR-451 Planktonic foraminifera >150 μm cm-2 yr-1
SU90-09 Planktonic foraminifera >150 μm g-1
b
GRIP Ca2+ (p.p.b.)
a
GRIP δ18O (‰)
Younger Dryas
Bølling warming
HE-sl1
Age (yr 1950 BP)

previous studies from the IRD belt (e.g., Bond et al., 1992; Broecker, 1994; Cortijo et al., 1997; Hemming, 2004), core SU90-09 has a maximum increase in surface water dilution with isotopically light freshwater from 17.4 to 16.7 ka BP, including a $\delta^{18}O_{npl}$ shift of −0.9‰ in just over 100 years at ~17.3 ka BP. This rapid shift followed more gradual freshening (−0.7‰ in 900 years), which started at ~18.3 ka BP. The number of lithic grains g^{-1} (IRD concentration) gradually increases at around the same time as the surface water dilution, with a pronounced maximum associated with the maximum freshwater dilution signal focussed at ~16.8 ka BP. This shows a 'typical' Heinrich event signature with meltwater derived from a massive iceberg discharge (e.g., Hemming, 2004). The number of planktonic foraminifera g^{-1} decreases from 8000 to a few hundred, with a minimum centred at the interval of maximum surface water dilution (17.4–16.7 ka BP), when *N. pachyderma* (left-coiling) became the dominant surface dweller (Grousset et al., 2001). Compared to core SU90-09, and to descriptions of Heinrich layers from the IRD belt (Bond et al., 1992, 1999; Grousset et al., 2000, 2001; see review of Hemming, 2004), records of $\delta^{18}O_{npl}$, IRD and planktonic foraminiferal fluxes from core TTR-451 (Eirik Drift) have distinctly different patterns and timings. Based on the generally low IRD flux during the main $\delta^{18}O_{npl}$ shift (Fig. 4d, e), this change does not seem to be primarily derived from an iceberg event. Instead, we interpret this $\delta^{18}O_{npl}$ shift during the H1 interval to have originated from iceberg-free freshened surface waters, similar to suggestions by van Kreveld et al. (2000).

On the basis of consistent ΔR estimates for the Younger Dryas from TTR-451 with those from the Norwegian margin (Bondevik et al., 2006), as well as the excellent agreement between the $\delta^{18}O_{npl}$ records on a purely radiocarbon chronology (see Supplementary Content 1), we use inferred TTR-451 ΔR values for H1 to convert ages for core MD95-2010 onto the GICC05 chronology. By using these inferred ΔR values for MD95-2010, a sharp increase in magnetic susceptibility values (identified by Dokken and Jansen (1999) as the Bølling warming) shifts from 15.5 ka BP on the Calib6.01 chronology, to 14.7 ka BP on the ΔR corrected age-scale (see Supplementary Content 1), corroborating this method.

Consonant with previous studies from the Nordic Seas (e.g., Duplessy et al., 1991; Rasmussen et al., 2002a, b; Rasmussen and Thomsen, 2004, 2008), the MD95-2010 $\delta^{18}O_{npl}$ and *Cassidulina teretis* ($\delta^{18}O_{ct}$) records an up to a −2‰ $\delta^{18}O_{npl}$ excursion (Dokken and Jansen, 1999) that spans the later phase of H1 (~16.5–~15 ka BP) (Fig. 4f). Comparison of $\delta^{18}O_{npl}$ records from Eirik Drift and the Nordic Seas (Fig. 4f) indicates that, apart from resolution differences, these records are nearly identical. This strongly indicates direct surface water communication between the Nordic Seas and Eirik Drift during H1. Unfortunately, abundances of benthic foraminifera are too low in TTR-451 to permit a comparable benthic $\delta^{18}O$ record from Eirik Drift.

Light $\delta^{18}O_{npl}$ and benthic $\delta^{18}O$ excursions, with nearly identical patterns, timing and magnitude to those in cores TTR-451 and MD95-2010, have been described for cores from the Nordic Seas, the northern North Atlantic (particularly the Faroe-Shetland Gateway), and around Eirik Drift (Vidal et al., 1998; Dokken and Jansen, 1999; Rasmussen et al., 2002a; Rasmussen and Thomsen, 2004; Lekens et al., 2005; Hillaire-Marcel and de Vernal, 2008; Meland et al., 2008). There are four hypotheses to explain this light $\delta^{18}O$ isotopic event. The first involves iceberg derived, low salinity meltwater pulses and halocline deepening (e.g., Hillaire-Marcel and Bilodeau, 2000; Rashid and Boyle, 2007). Based on the low H1 IRD flux in core TTR-451 from Eirik Drift, we consider this first hypothesis to be unlikely. The second hypothesis involves a reversed thermocline as a result of sea-surface capping with freshwater and sea-ice, and warming of the subsurface layer (e.g., Mignot et al., 2007; Peck et al., 2008). However, $\delta^{18}O$ measurements on *N. pachyderma* sub-populations (based on size) from core MD95-2024 (Labrador Sea) reveal a negative temperature gradient along the thermocline, which led Hillaire-Marcel and de Vernal (2008) to reject this second hypothesis. The third hypothesis involves the sinking of isotopically light brines as a result of intense sea ice formation (e.g., Vidal et al., 1998; Dokken and Jansen, 1999; Risebrobakken et al., 2003; Millo et al., 2006; Hillaire-Marcel and de Vernal, 2008; Meland et al., 2008). The fourth hypothesis suggests penetration of relatively warm (4–8 °C) waters into the Nordic Seas at intermediate depths (<1700 m), which is suggested to represent the North Atlantic Drift (NAD) that flowed below the ocean surface into the Nordic Seas (Rasmussen and Thomsen, 2004). We use our new records from Eirik Drift to evaluate these latter two hypotheses.

4.3. *$\delta^{18}O$ excursions during H1 in the Nordic Seas and at Eirik Drift*

We first consider the sea-ice hypothesis for generating the light $\delta^{18}O$ excursion in planktonic and benthic foraminifera in the Nordic Seas and in planktonic foraminifera at Eirik Drift during H1. LGM reconstructions for the northern North Atlantic suggest that seasonal sea-ice likely extended down to ~40°N (Mix et al., 2001; Pflaumann et al., 2003). However, a regional $\delta^{18}O_{npl}$ of ~+4.5‰ indicates that the Nordic Seas and northern North Atlantic likely were sea-ice free in summer (e.g., Weinelt et al., 1996, 2003; de Vernal et al., 2002; Meland et al., 2005; Millo et al., 2006). High sedimentation rates, high planktonic foraminiferal fluxes and relatively heavy $\delta^{18}O_{npl}$ records from western Fram Strait suggest that seasonally 'open' conditions even extended to this region during the LGM, unlike the permanently sea-ice covered central Arctic Ocean region, where both sedimentation rates and planktonic foraminiferal abundances were considerably lower (Nørgaard-Pederson et al., 2003). Because of the relatively high numbers of planktonic foraminifera per gram, despite the high sedimentation rate in core MD95-2010, we suggest that seasonally open conditions likely prevailed throughout the time period of H1in the Nordic Seas.

Dokken and Jansen (1999) proposed that freshwater additions into the North Atlantic and AMOC weakening would have resulted in high-latitude cooling and rapid extension of the sea-ice margin across the Nordic Seas during H1. Sea-ice forms with little oxygen isotope fractionation from freezing surface waters, which at this time were affected by freshwater dilution, so that the rejected

Fig. 4. a. GRIP ice core $\delta^{18}O$ record plotted versus the GICC05 timescale (Rasmussen et al., 2006, 2008; Andersen et al., 2006; Svensson et al., 2006; Vinther et al., 2006). b. Concentration of Ca^{2+} (p.p.b.) in the GRIP ice core (Fuhrer et al., 1993; Rasmussen et al., 2006, 2008; Andersen et al., 2006; Svensson et al., 2006). c. Records of the flux of planktonic foraminifera >150 μm $cm^{-2}\ yr^{-1}$ for core TTR-451 (black) and the number of planktonic foraminifera >150 μm per gram of dry sediment for core SU90-09 (green). d. Records of the flux of ash free lithic grains $cm^{-2}\ yr^{-1}$ (pink) and total lithic grains $cm^{-2}\ yr^{-1}$ (black) for core TTR-451. The number of lithic grains >150 μm per gram of dry sediment for core SU90-09 (green). e. $\delta^{18}O_{npl}$ records for TTR-451 (black) and SU90-09 (green) f. $\delta^{18}O_{npl}$ records for TTR-451 (black) and MD95-2110 (blue). $\delta^{18}O_{ct}$ is shown in orange. The bright green line represents the timing of extreme rates of sediment deposition in the Nordic Seas (Lekens et al., 2005), and the purple line shows the timing of the Norwegian Channel Ice Stream retreat (Nygård et al., 2004). The black star indicates the timing of the termination of the Bremanger event (Nygård et al., 2004). g. κ_{ARM}/κ for Eirik Drift core TTR-451 (black). κ_{ARM}/κ data for TTR-451 are presented alongside the $^{231}Pa/^{230}Th$ record of core GGC5 from Bermuda Rise (red) (McManus et al., 2004). κ_{ARM}/κ reflects variations in magnetic mineral grain size (Banerjee et al., 1981; Verosub and Roberts, 1995), transported by Proto-NADW from a single source of fine-grained minerals, the Nordic Basaltic Province (Kissel et al., 1999, 2009; Laj et al., 2002).

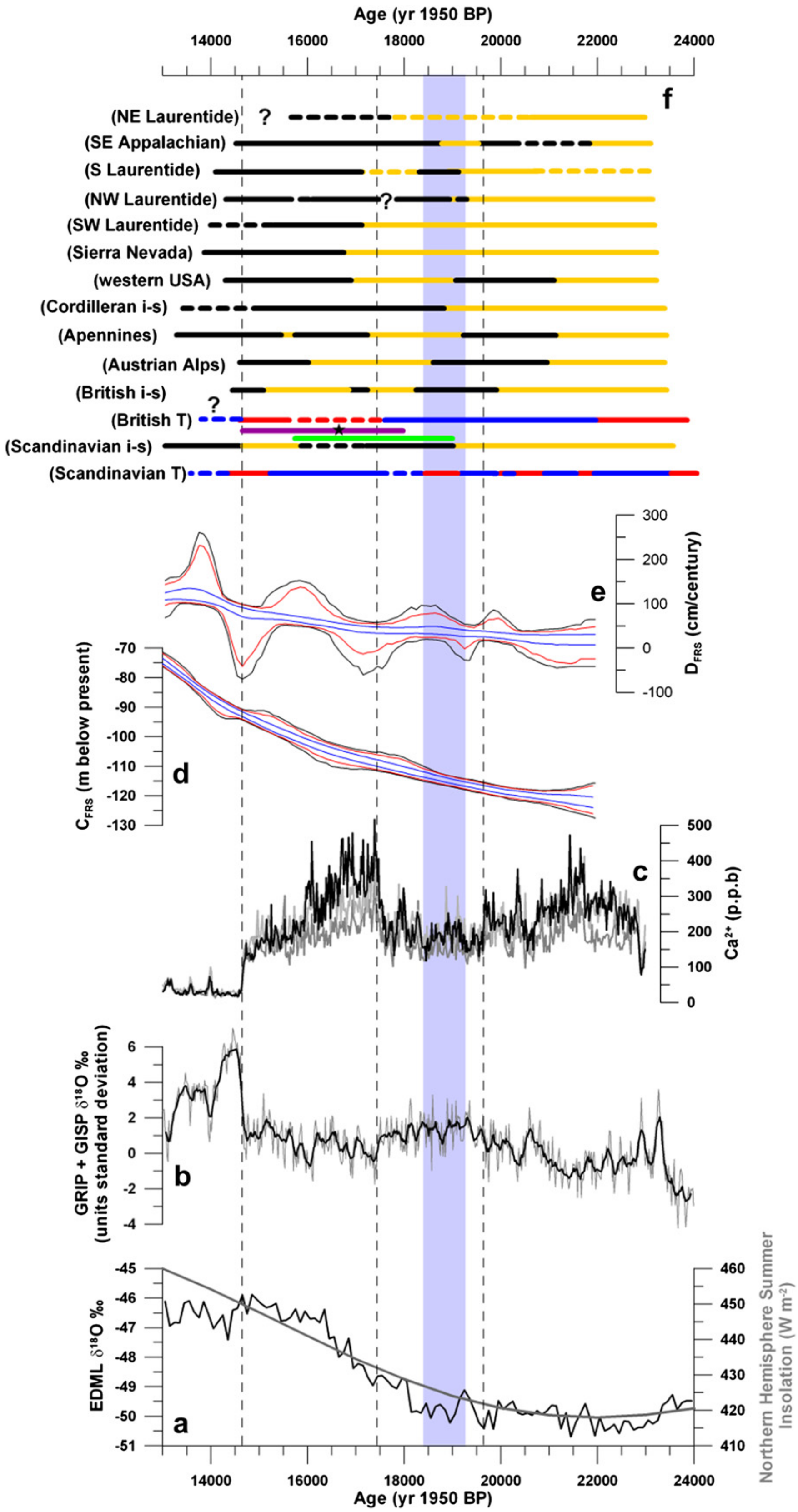

Fig. 5. a. The EDML $\delta^{18}O$ record (black) on the GICC05 time scale (EPICA Community Members, 2006) and the northern hemisphere summer (July) insolation (grey) at 65°N (Berger, 1991, 1999). b. The GRIP + GISP2 composite/mean $\delta^{18}O$ ice core record in unit standard deviation on the GICC05 timescale. c. The concentration of Ca^{2+} (p.p.b.) in the Greenland ice cores. GRIP is shown in black, GISP2 in dark grey and NGRIP in light grey (Fuhrer et al., 1993; Mayewski et al., 1994; Bigler, 2004; Rasmussen et al., 2006, 2008). d. C_{FRS} is the combined far-field relative sea-level record and in panel (e) the D_{FRS} record shows the first derivative of the sea-level change (rate of sea-level change). These records were constructed using a Monte Carlo statistical analysis after Stanford et al. (in press). The 67%, 95%, and 99% probability intervals for the deglacial sea-level history are shown in blue,

brines would have advected a relatively low $\delta^{18}O$ signal to deeper waters. Dokken and Jansen (1999) and Meland et al. (2008) suggested that brine rejection would result in convection of 'pooled' isotopically light surface waters to intermediate depths (to the base of the halocline), thereby accounting for the light H1 $\delta^{18}O$ signal in both surface waters and at intermediate depths. On the basis of similar $\delta^{18}O$ trends, Dokken and Jansen (1999) extended this hypothesis to account for $\delta^{18}O$ distributions in the Nordic Seas during other Heinrich events (Fig. 6). However, comparison of $\delta^{18}O_{npl}$ and $\delta^{18}O_{ct}$ data from the Nordic Seas for Heinrich events 4 and 6 (Fig. 6) indicates a larger $\delta^{18}O$ shift to lighter values at intermediate depths (benthics) than for surface waters (planktonics). For Heinrich event 6 (H6), this difference in $\delta^{18}O$ shift is approximately double. Furthermore, $\delta^{18}O_{ct}$ shifts to lighter values some 400 yrs prior to $\delta^{18}O_{npl}$. This timing offset is even more pronounced for H3 in core ENAM93-21 from the southern Nordic Seas (Dokken and Jansen, 1999). Because sea-ice formation and resultant brine rejection mix the light $\delta^{18}O$ signal in the halocline from the surface down through the water column, greater freshening would be expected in $\delta^{18}O_{npl}$ than in $\delta^{18}O_{ct}$. Also, if there were any temporal offsets, then $\delta^{18}O_{npl}$ would shift to lighter values before the $\delta^{18}O_{ct}$. The observations (Fig. 6) are therefore not consistent with the mechanism invoked by Dokken and Jansen (1999). Furthermore, core TTR-451 records nearly identical absolute $\delta^{18}O_{npl}$ as core MD95-2010 (Fig. 4f). Therefore, nearly instantaneous and rapid growth of the seasonal sea-ice margin would be needed across the entire Nordic Seas and northern North Atlantic to account for these observations. Such rapid and instantaneous sea-ice growth across such a vast area may have occurred (e.g., Gildor and Tziperman, 2003). However, open ocean convection would have likely resulted in dilution of the $\delta^{18}O$ signal. In order to generate brines dense enough to sink to intermediate depths and with such a low $\delta^{18}O$ signal, seasonal sea-ice is required to have formed in shallow shelf areas, reducing the $\delta^{18}O$ dilution because of limited mixing depths, and the Barents Sea Shelf may have provided such a location (Bauch and Bauch, 2001). However, Bauch and Bauch (2001) considered this scenario to be unlikely since the rates of sea ice formation would have been unrealistically high, and furthermore, the GLAMAP LGM reconstruction (Pflaumann et al., 2003) suggests that the Barents Shelf region was permanently sea-ice covered. A recent study by Rasmussen and Thomsen (2010) in Storfjorden, Svalbard, in the Barents Sea showed that, at present, brines that can attain a high enough density to sink to intermediate depths are those formed from cold, saline waters, not freshwaters. Furthermore, these brines have high $\delta^{18}O$ and $\delta^{13}C$ values, as opposed to the strongly light and low values recorded during H1. On the basis of these arguments, we reject the hypothesis that brine rejection from sea-ice formation caused the transfer of the light $\delta^{18}O_{npl}$ excursion to $\delta^{18}O_{ct}$ in the Nordic Seas.

We now consider the fourth hypothesis that has been put forward to account for the observed light $\delta^{18}O$ isotopic excursions in the Nordic Seas. Rasmussen et al. (1996a, b) and Rasmussen and Thomsen (2004) found that in a number of cores (including ENAM93-21) from the Nordic Seas and the Faroe-Shetland Gateway, there is a distinct abundance increase in the benthic foraminiferal 'Atlantic species' group (e.g., *Sigmoilopsis schlumbergi*, *Egerella bradyi*, *Alabaminella weddellensi*, *Epistominella decorata*, *Bulimina costata*, *Sagrina subspinescens*, *Gyroidina* spp.) at the same time as the H1 $\delta^{18}O_{npl}$ and $\delta^{18}O_{ct}$ light excursion in the Nordic Seas. Similar to Bauch and Bauch (2001), Rasmussen and Thomsen (2004) suggested that there was a weak subsurface invasion of relatively warm (4–8 °C) Atlantic waters (below 1 km) into the Nordic Seas during H1, which they interpreted as a subsurface expression of the NAD. Abundance differences of the 'Atlantic species' group have been used to infer that temperatures at intermediate water depths were greater in the Nordic Seas during the latter part of H1 than during Dansgaard-Oeschger interstadials (Rasmussen and Thomsen, 2004). Rasmussen and Thomsen (2004) suggested that the benthic and planktonic $\delta^{18}O$ shift to lighter values in the Nordic Seas during H events was due to this subsurface invasion of relatively warm water.

Similar to Meland et al. (2008), we find the interpretation of Rasmussen and Thomsen (2004) problematic because relatively warm inflowing waters would have needed to become denser to enter the Nordic Seas at water depths greater than 1 km. Meland et al. (2008) also suggested that although model experiments indicate that deep waters may be warmed by a few °C (Weaver et al., 1993; Winton, 1997; Paul and Schulz, 2002), they do not account for the shallow Iceland-Scotland Ridge that these waters would need to cross. Moreover, Meland et al. (2008) noted that benthic foraminiferal Mg/Ca for core MD95-2010 do not indicate increased temperatures at intermediate depths in the Nordic Seas during this time period (Dokken and Clark, unpublished data). Furthermore, relatively large temporal offsets are apparent for nearly all Nordic Sea cores between the peak 'Atlantic species' abundances and the $\delta^{18}O$ minima (Rasmussen and Thomsen, 2004). Our observation of identical absolute $\delta^{18}O_{npl}$ in cores TTR-451 and MD95-2010 strongly suggests that there was direct water mass communication between the Nordic Seas and Eirik Drift during H1. If the light $\delta^{18}O$ excursion in the Nordic Seas resulted from relative warming of waters, then it would be unlikely to be expressed nearly identically outside the enclosed Nordic Seas at Eirik Drift. Finally, it is widely accepted that both the Denmark Strait and Iceland Scotland Ridge overflows had ceased (McManus et al., 2004; Hall et al., 2006; Stanford et al., 2006). Therefore, to accommodate inflow, waters are needed to have out-flowed at the surface from the Nordic Seas. Given the large isotopic shift observed across the Nordic Seas, a large body of inflowing waters would have been needed, and we question whether an equivalent volume of outflowing surface waters would have been likely.

Given that the Nordic Seas deep overflows had more or less collapsed from ~17.5 ka BP (Fig. 4g), and that the Bering Strait (at a present water depth of ~50 m) was closed due to low sea level (−110 m), any exchange between the Nordic Seas and North Atlantic, to maintain mass balance in the Nordic Seas, would have been via surface waters (e.g., via the Denmark Strait by means of the EGC). Hence, we suggest that $\delta^{18}O_{npl}$ signals observed at Eirik Drift resulted from net freshwater (diluted surface water) export from the Nordic Seas, in a configuration reminiscent of modern Arctic outflow through the Fram Strait. This would explain the close signal similarity of absolute values between $\delta^{18}O_{npl}$ in the Nordic Seas and over Eirik Drift.

We conclude that neither the sea-ice nor the subsurface warming hypotheses (Dokken and Jansen, 1999; Rasmussen and

red and black, respectively. The blue shaded area indicates the timing of an apparent rapid sea-level rise at ~19 ka BP. f. Recalibrated temperature records from Scandinavia (Alm, 1993) and Britain (Atkinson et al., 1987); blue = cold, blue dashed = gradual cooling, red = warm, and red dashes = gradual warming. Yellow lines indicate glacial advances, and retreats are shown in black. Dashed lines are where there are no datings. Data are after Marks (2002), Rinterknecht et al. (2006), McCabe and Clark (1998), McCabe et al. (2007), Bowen et al. (2002), Giraudi and Frezzotti (1997), Clague and James (2002), Licciardi et al. (2004), Dyke et al. (2002) and references therein, and Ivy-Ochs et al. (2006). The green line represents the timing of extreme rates of sediment deposition in the Nordic seas (Lekens et al., 2005) and the purple line shows the timing of the Norwegian Channel Ice Stream retreat (Nygård et al., 2004). The black star indicates the timing of the termination of the Bremanger event (Nygård et al., 2004). All raw and calibrated datings are provided in the Supplementary Content 2.

Table 2
Timings of terrestrial climate change and glacial movements from the LGM to the Bølling warming.

Timing	Paleo-climate description	Evidence	References
~26 − 21 ka BP (LGM)	Ice-sheets at maximum extent	Barbados, Sunda Shelf and Boneparte Gulf sea-level records	Fairbanks (1989), Bard (1990a; b), Hanebuth et al. (2000; 2009), Yokoyama et al. (2000), Lambeck et al. (2002), Fairbanks et al. (2005) Peltier and Fairbanks (2006), Stanford et al. (in press), Fig. 5d, e
		Datings on terminal moraines	Bowen et al. (2002), Dyke et al. (2002), Rinterknecht et al. (2006), Fig. 5f
	Relative cooling in Greenland.	GRIP and GISP2 $\delta^{18}O$ ice core records	See 3.1 for discussion, Fig. 5b
	Relative warmth in Britain and Scandinavia	*Coleoptera* abundances and pollen records	Alm (1993), Atkinson et al. (1987), Fig. 5f
~21-19 ka BP	Warming in Greenland	GRIP and GISP2 $\delta^{18}O$ ice core records	Fig. 5b
	Increased Northern Hemisphere summer insolation		Berger (1991), Fig. 5a
	Warming in Antarctica	EDML $\delta^{18}O$ ice core records	EPICA community members (2006), Fig. 5a
	Southern hemisphere warming	Marine sediment core records	Arz et al. (1999), Sachs et al. (2001), Kim et al. (2002)
	British and Laurentide ice sheets underwent the first retreat from their LGM position	Boulder exposure ages and datings on terminal moraines	Bowen et al. (2002), Dyke et al. (2002) and references therein, Fig. 5f
		Increased branched and isoprenoid tetraether (BIT)-index in the Bay of Biscay at ~19.5 ka BP supports the dating of the British ice-sheet retreat.	Menot et al. (2006)
	Glaciers in the Austrian Alps, Apennines, and western North America also started to retreat.	Boulder exposure ages and datings on terminal moraines	Giraudi and Frezzotti (1997), Licciardi et al. (2004), Ivy-Ochs et al. (2006), Fig. 5f
	Cooling across Scandinavia	Pollen data	Alm (1993)
	Rapid cooling in the British Isles	Disappearance of *Coleoptera*	Atkinson et al. (1987)
~19 − 17.5 ka BP	From around 19 − 18 ka BP: Brief warming in Scandinavia	Pollen records	Alm (1993)
	From 19 ka BP: The Scandinavian ice-sheet undergoes a sustained retreated.	Datings on terminal moraines	Marks (2002), Rinterknecht et al. (2006), Fig. 5f
		Marine sediment records	Bauch et al. (2001)
	This coincides with the deposition of fine-grained sediments over a >1600 km^3 area of the Nordic Seas.	Sediment cores and seismic mapping	Hjelstuen et al. (2004), Lekens et al. (2005)
	Penecontemporaneous glacial retreats are also documented for the northwest American Cordilleran ice sheet, the southeast Appalachian margin and the Austrian Alps. The ~500 yr duration Eerie interstadial is also dated at ~18.8 ka BP in the southern Laurentide region.	Boulder exposure ages and datings on terminal moraines	Clague and James (2002), Dyke et al. (2002) and references therein, Ivy-Ochs et al. (2006), Fig. 5f
	On a global scale, ice volume appears to have begun a first substantial decrease, as suggested by an initial rapid step in sea-level rise	Sunda Shelf and Boneparte Gulf sea-level records	Hanebuth et al. (2000; 2009), Yokoyama et al. (2000), Stanford et al. (in press), Fig. 5d, e
	However, between 19.5 and 18.5 ka BP, the British ice sheet re-advanced in response to cooling.	Lack of ^{36}Cl boulder exposure ages	Bowen et al. (2002)
		AMS ^{14}C datings of marine mud	McCabe and Clark (1998), McCabe et al. (2007) and references therein
	19.3 ka BP to ~17 ka BP: Glacial advance in the Apennines	Boulder exposure ages and datings on terminal moraines	Giraudi and Frezzotti (1997)
	~18 ka BP: Initiation of glacial advance within the southern Laurentide region	Boulder exposure ages and datings on terminal moraines	e.g., Dyke et al. (2002)
~19 − 17.5 ka BP	From around 18.3 ka BP, the rate of sea-level rise decreased	Sunda Shelf, Barbados and Boneparte Gulf sea-level records	Fairbanks (1989), Bard (1990a; b), Hanebuth et al. (2000; 2009), Yokoyama et al. (2000), Lambeck et al. (2002), Fairbanks et al. (2005) Peltier and Fairbanks (2006), Stanford et al. (in press) Fig. 5d, e
17.5 − 15.5 ka BP	From17.5 ka BP: Rapid intensification of polar atmospheric circulation and/or a change in circulation patterns, occurred along with minor cooling in Greenland	Sharp increase in the Ca^{2+} ion concentration in the Greenland ice cores and decreased Greenland ice core $\delta^{18}O$	Biscaye et al. (1997), Mayewski et al. (1997), Rohling et al. (2003), Andersen et al. (2006), Svensson et al. (2006), Rasmussen et al. (2006; 2008) and references therein, Jullien et al. (2006), Fig. 5a, b
	From 17.5 ka BP: Significant glacial retreat occurred on a nearly global scale. Ice-free conditions in the Gulf of St. Lawrence by ~16.7 ka BP indicate the scale of this retreat at the southeastern Laurentide margin, and a drawdown of the ice centre around the Hudson Bay region is thought to reflect important reorganisation of ice-streams	Boulder exposure ages and datings on terminal moraines	Giraudi and Frezzotti (1997), McCabe and Clark (1998), Denton et al. (1999), Dyke et al. (2002) and references therein, Bowen et al. (2002) Clague and James (2002) Licciardi et al. (2004), Ivy-Ochs et al. (2006), Rinterknecht et al. (2006), McCabe et al. (2007), Fig. 5f
	Contrary to the cooling trend in Greenland ice cores, slight amelioration in British climate at ~17.5 ka BP	Re-appearance of *Coleoptera*. Species abundances indicate that temperatures were similar to those at the LGM (winter temperatures of around -25 °C)	Atkinson et al. (1987)
	17.5 ka BP: Ice sheet retreat in the British Isles, but it re-advance back to near its LGM extent by 16.5 ka BP. In the Apennine region, a shorter duration re-advance occurred at around 15.5 ka BP	Datings on terminal moraines	McCabe and Clark (1998), McCabe et al. (2007), Ivy-Ochs et al. (2006), Giraudi and Frezzotti (1997)
	From 16.2 ka BP: Atmospheric polar circulation intensity decreased slightly at this time, although it remained relatively intense, however, temperatures over Greenland did not significantly improve	Gradual decrease in the Ca^{2+} ion concentration in the Greenland ice cores and light Greenland ice core $\delta^{18}O$	Biscaye et al. (1997), Mayewski et al. (1997), Rohling et al. (2003), Andersen et al. (2006), Svensson et al. (2006), Rasmussen et al. (2006; 2008) and references therein, Jullien et al. (2006), Fig. 5a, b

15.5 – 14.6 ka BP	Significant climate amelioration is observed for the British Isles and ice retreat from the H1 maximum extent was well underway on a nearly global scale	*Coleoptera* abundances	Atkinson et al. (1987)
	The southern Scandinavian ice sheet, however, re-advanced at ~15.5 ka BP, most likely due to a positive mass balance related to increased moisture availability	Boulder exposure ages and datings on terminal moraines	Giraudi and Frezzotti (1997), Benson et al. (1998), McCabe and Clark (1998), Clague and James (2002), Dyke et al. (2002) and references therein, Ivy-Ochs et al. (2006) McCabe et al. (2007), Hendy and Cosma (2008)
	However, in Scandinavia and Greenland temperatures remained low	Boulder exposure ages and datings on terminal moraines	Rinterknecht et al. (2006)
		Pollen records and light Greenland ice core $\delta^{18}O$	Alm (1993), Andersen et al. (2006), Svensson et al. (2006), Rasmussen et al. (2006; 2008)
14. 6 ka BP	Greenland temperatures are estimated to have risen by more than 10 °C and ice-sheets rapidly retreated on a global scale.	Greenland ice core $\delta^{18}O$ records	Severinghaus and Brook (1999), Andersen et al. (2006), Svensson et al. (2006), Rasmussen et al. (2006; 2008)
		Boulder exposure ages and datings on terminal moraines	Giraudi and Frezzotti (1997), Benson et al. (1998), McCabe and Clark (1998), Clague and James (2002), Dyke et al. (2002) and references therein, Ivy-Ochs et al. (2006) McCabe et al. (2007), Hendy and Cosma (2008)
	Sharp climatic improvements in low latitude proxy records	e.g., Marine sediment cores from Cariaco Basin and speleothem data from Hulu Cave.	Hughen et al. (1996), Wang et al. (2001), Lea et al. (2003)

Thomsen, 2004) can satisfactorily explain $\delta^{18}O$ patterns within the Nordic Seas during H1. We therefore develop an alternative explanation for the light $\delta^{18}O$ excursion within the Nordic Seas, which then extended over Eirik Drift.

4.3.1. A new hypothesis for light $\delta^{18}O$ excursions during H1 in the Nordic Seas and at Eirik Drift

Seismic mapping and studies of marine cores have revealed that sediment accumulation rates were high within the Nordic Seas during H1 (Hjelstuen et al., 2004; Sejrup et al., 2004; Lekens et al., 2005). Core MD99-2291 from the Vøring Plateau, southeastern Norwegian Sea, contains laminated/partly laminated fine-grained clay and silt (individual laminae are between 1 mm and 150 mm thick), with generally low planktonic foraminiferal abundances and occasional IRD (Lekens et al., 2005). Covering an area of ~1600 km^2 on the Norwegian Sea floor, these post ~18.6 ka BP sediments have a volume of ~1000 km^3 and attain a thickness that can exceed 20 m (Hjelstuen et al., 2004; Sejrup et al., 2004; Lekens et al., 2005). However, since the Storegga Slide (*ca* 8.2 ka BP; Bugge et al., 1987; Bondevik et al., 1997, 2003) removed much of this deposit, calculations of total sediment volume are problematic (Hjelstuen et al., 2004; Sejrup et al., 2004; Lekens et al., 2005).

$\delta^{18}O_{npl}$ data from these sediments have the same absolute values as those in MD95-2010 and TTR-451, and the termination of the laminated deposits at 15.1 ka BP is coincident with peak light $\delta^{18}O_{npl}$ in the Nordic Seas (Lekens et al., 2005). Given the similar timing of emplacement of these sediments and rapid retreat of the Fennoscandian ice sheet (e.g., Rinterknecht et al., 2006), Lekens et al. (2005) suggested that the sediments had a meltwater origin. Based on the presence of >2 mm IRD and pristine fully articulated bivalves, Lekens et al. (2005) suggested that they were deposited hemipelagically, and classified them as ‘plumites’ (i.e., sediments deposited during surface freshwater events). Lekens et al. (2005) also tentatively suggested that the laminations, which comprise two units (dark fine-grained laminae and lighter coloured coarser-grained laminae), represent winter sea-ice cover and summer plume deposition, respectively. Based on the detailed sediment descriptions provided by Lekens et al. (2005), and the volume of sediment that was delivered into the Nordic Seas over a relatively short time interval (over 1000 km^3 in ~2000 yrs), we question whether the sediments resulted from fall-out from surface waters. Instead, due to the relatively high sediment concentrations within the meltwater plumes, we suggest that it is more likely that the sediments entered the Nordic Seas below the sea surface (e.g., Fohrmann et al., 1998), and that they therefore represent low-velocity hyperpycnal deposits that resulted from glacial melting and outwash.

A hyperpycnal flow is a negatively buoyant flow that travels along the basin floor because its density is greater than that of the ambient water mass into which it is injected, and it attains its density from the entrained sediment load (Mulder and Syvitski, 1995; Stow, 1996). This process means that terrestrial material can be transported directly into marine environments via turbulent flow, initially with a freshwater origin (Mulder et al., 2003). Hyperpycnal flows can carry sediments finer than medium sand over large distances (Mulder et al., 2003). Hyperpycnites (the deposits from hyperpycnal flows) can be generated today from ‘dirty’ rivers, flood events, dam breaks, or Jökulhaups. Lekens et al. (2005) rejected the possibility that these sediments represent subsurface turbidity current generated deposits based on the rhythmic nature of the sediments, a lack of erosional contacts, and the presence of fully articulated bivalves and IRD (Rashid et al., 2003). However, the low-velocity, quasi-steady regime of hyperpycnal flows from low-velocity floods may not have erosional contacts (Mulder et al., 2003), and we suggest that such processes do not preclude the occurrence of IRD or intact bivalves.

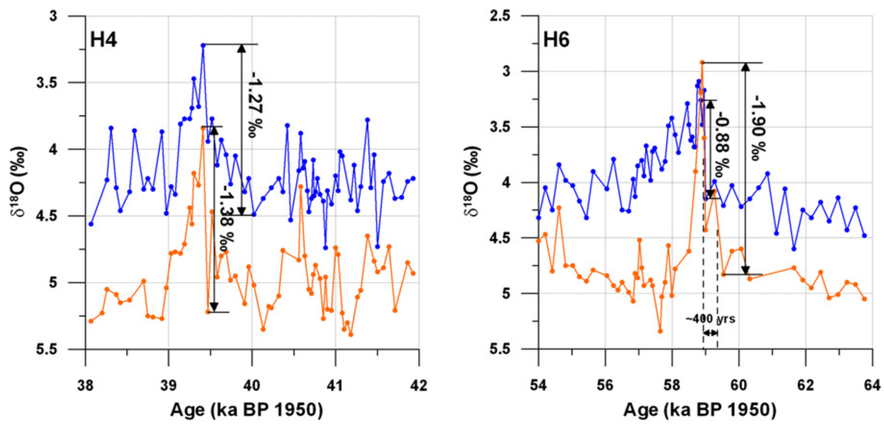

Fig. 6. Benthic (orange) and planktonic (blue) δ^{18}O records for core MD95-2010 for H4 (left) and H6 (right). The records are generated from *C. teretis* (benthic foraminifera) and *N. pachyderma* (left coiling) (planktonic foraminifera) (data from Dokken and Jansen, 1999).

Hyperpycnites that form at river mouths during floods are characterised by two units; a coarsening-upward sequence as discharge increases, followed by a fining-upward unit as discharge wanes (Mulder et al., 2001, 2003). We suggest that the rhythmic, laminated deposits described by Lekens et al. (2005) may represent annual changes in flow regime, with the lighter coloured coarser-grained portions resulting from high summer melt discharges. Similar laminated sedimentary sequences, which contain relatively large IRD concentrations, have been described for H1 from the northwestern Bay of Biscay (Zaragosi et al., 2001), and from the North Atlantic (Hesse et al., 1996, 2004; Hesse and Khodabakhsh, 1998), where they were interpreted as hyperpycnal deposits that resulted from sediment-laden meltwater from the European and Laurentide ice-sheets, respectively. Similar sequences have also been described in deglacial infill of an East Greenland fjord (Hansen, 2004).

Hyperpycnal freshwater delivery into the Nordic Seas provides a mechanism for supplying low δ^{18}O meltwaters to intermediate depths. As the hyperpycnal flows de-watered, relatively fresh, low density, buoyant meltwaters would have risen toward the surface (while strongly mixing with ambient waters) (e.g., Hansen, 2004), which would have caused planktonic δ^{18}O anomalies similar to the benthic δ^{18}O anomalies. A hyperpycnal mechanism for delivering freshwater allows the observed greater magnitude and earlier timing of the δ^{18}O shift in the benthic versus the planktonic data because the relatively freshwater would have been mixed upward from depth, rather than downward from the surface. We note, however, that the basal date of the thick Nordic Sea deposits suggests that deposition started ~1000 yrs prior to the light $\delta^{18}O_{npl}$ excursion (bright green line in Fig. 4f). Similarly high rates of sedimentary deposition are also observed on the North Sea Fan at around the timing of the Nordic Seas δ^{18}O anomaly. Submerged moraines, scour marks and glacial bedforms indicate the extent of the Norwegian Channel Ice Stream (NCIS) and regional ice margin (e.g., Sejrup et al., 2000; Nygård et al., 2004; see purple line in Figs. 4 and 5). At around 16.7 ka BP (re-calibrated here using Calib6.01; black star in Figs. 4 and 5), the NCIS margin made a significant and final retreat from its Bremanger (H1) event position back to the coastline (Nygård et al., 2004; Lekens et al., 2005), suggesting a maximum freshwater event at around that time. An alternative explanation for the apparent 1000 yr 'mismatch' may be inferred from the description of core MD99-2291 (Lekens et al., 2005), which indicates a sediment coarsening with fewer laminations, increased planktonic foraminifera concentrations, and decreased sedimentation rates, coincident with the $\delta^{18}O_{npl}$ event onset in the same core. This may indicate an increased rate of meltwater injection into the Nordic Seas, with sediments reflecting more proximal material.

Based on modern rivers that produce at least one hyperpycnal flow each year, Mulder and Syvitski (1995) estimated the critical threshold particle concentration required for a water mass to plunge subsurface. Calculated values range from ~38.9 kg m^{-3} for low latitude rivers to ~43.5 kg m^{-3} at high latitudes. Measured annual average suspended particle concentrations are, however, somewhat lower (e.g., 20.7 kg m^{-3} for the Rioni in Russia) as hyperpycnal flows occur during peak discharge. Mulder et al. (2003) suggested that rivers with initial suspended particle threshold concentrations as low as 5 kg m^{-3} can produce hyperpycnal flows during flood.

We test the hypothesis that meltwaters may have entered the Nordic Seas hyperpycnally during H1 by calculating average suspended particle concentrations, assuming that the sediments have a particle density of quartz, 2650 kg m^{-3} (Mulder and Syvitski, 1995). We calculate this for three scenarios, and consider mixing this sediment load with incrementally increasing freshwater volumes. Scenario 1 involves the minimum estimated volume of sediment deposited during H1 in the Nordic Seas (1000 km^3; Hjelstuen et al., 2004; Sejrup et al., 2004; Lekens et al., 2005). Scenario 2 takes into account that the light δ^{18}O anomaly in MD99-2291 only spans the upper 1.4 m of the 10.5-m-thick laminated section. We therefore reduce the 1000 km^3 sediment volume by 87%. The Storegga Slide, which post-dated H1 by nearly 8000 years, removed a large proportion of the H1 deposits in the Norwegian Sea and therefore, the cited 1000 km^3 volume for the H1 deposit is a minimum estimate (Hjelstuen et al., 2004; Sejrup et al., 2004; Lekens et al., 2005). Although unrealistic, in scenario 3 we calculate the maximum possible sediment load of the H1 meltwaters by including the sediment volume contained within the Storegga Slide (3500 km^3; Bondevik et al. (2003)). Therefore, scenario 3 has a total sediment volume of 4500 km^3. Results are given in Table 3, and mixing curves for scenarios 1 and 2 are shown in Fig. 7.

Assuming that the -1.45‰ $\delta^{18}O_{npl}$ shift at Eirik Drift ($(\delta_{npl})_{Eirik}$) represents a mixed signal out of the Nordic Seas, we use a glacial meltwater end member δ^{18}O value of -35‰ ($\delta^{18}O_{MW}$) to calculate the volume of freshwater that likely entered the Nordic Seas during H1. A volume of 2145900 km^3 (V_{NS}) is used for the Nordic Seas, as we assume that mixing was constrained to the Norwegian Sea, Iceland Sea, and only the southernmost sector of the Greenland Sea (Nørgaard-Pederson et al., 2003), and we subtract the volume associated with a -110 m sea-level change. $(\delta_{npl})_{Eirik}$ is solved from the equation below, where δ_{NS} is the initial δ^{18}O value of $\delta^{18}O_{npl}$ in the Nordic Seas and at Eirik Drift and V_{MW} is the volume of

Table 3
Volumes of freshwater required to be mixed with sediment for meltwaters to plunge subsurface.

	Volume of sediment (km^3)	Volume of freshwater (km^3)	Equivalent global sea-level rise (m)	C_c ($kg\ m^{-3}$)
Scenario 1	1000	61009 (C^1)	0.169	43.5 (A^1)
Scenario 2	133	8303 (C^4)	0.023	43.5 (A^1)
Scenario 3	1000 + 3500 (Storegga)	273999	0.759	43.5

That is, for average suspended particle loads to exceed the critical particle concentration (C_c). $C_c = 43.5\ kg\ m^{-3}$ (Mulder and Syvitski, 1995; Mulder et al., 2003). In brackets are points denoted in Fig. 7.

meltwater. We calculate that V_{MW} equals ~89000 km^3, or the equivalent of 0.246 m of global sea-level rise.

$$\left(\delta_{npl}\right)_{Eirik} = [(V_{NS} \times \delta_{NS}) + (V_{MW} \times \delta_{MW})]/(V_{NS} + V_{MW}) \qquad (1)$$

We then consider a mixture of the derived volume of meltwater (V_{MW}) with sediment loads used in scenarios 1, 2 and 3 (Table 4, with mixing curves for scenarios 1 and 2 in Fig. 7), where the meltwater injection volumes are translated to equivalent global sea-level rise.

For scenario 1, a meltwater volume of 61009 km^3 is required for the flow to acquire the critical threshold particle concentration of 43.5 $kg\ m^{-3}$ (Table 3). Mixing 1000 km^3 of sediment with the calculated meltwater volume yields an average suspended particle concentration of nearly 30 $kg\ m^{-3}$ (Table 4), which is similar to the observed average suspended particle concentrations of modern high-latitude rivers that produce hyperpycnal flows (Mulder et al., 2003). For this scenario, meltwaters injected into the Nordic Seas during H1 could have done so hyperpycnally.

Scenario 2, with the 87% reduced sediment estimate, requires a meltwater volume of only 8303 km^3 for the sediment load to cause meltwater flow to exceed its critical particle concentration (43.5 $kg\ m^{-3}$) (Table 3). This volume is an order of magnitude less than the calculated meltwater volume (V_2). Mixing the relatively small sediment volume for scenario 2 with the calculated meltwater volume gives an average suspended particle concentration of 3.98 $kg\ m^{-3}$, which is less than the required >5 $kg\ m^{-3}$ reported by Mulder et al. (2003). However, for scenario 2, a minimum sediment load is mixed with a maximum meltwater volume, and is averaged over ~1000 yrs; therefore, sedimentation rates may have been

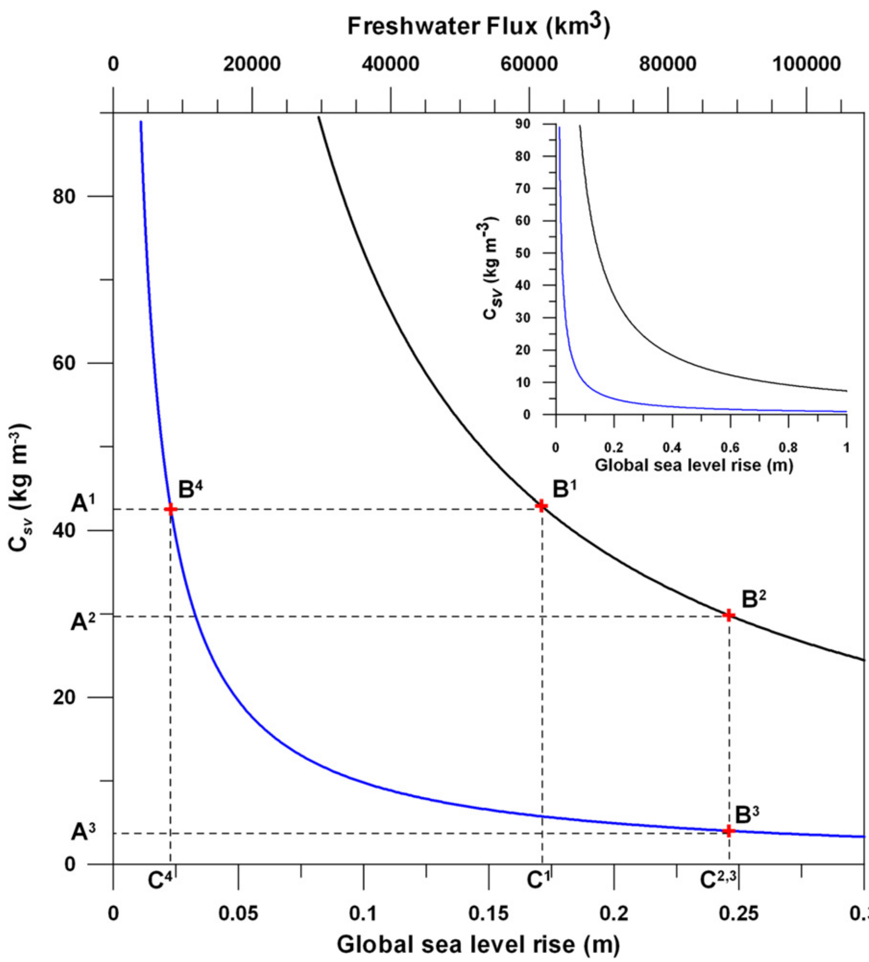

Fig. 7. Meltwater volume, in terms of its contribution to global sea-level rise, versus its average suspended particle concentration values (C_{sv}) for scenarios 1 (black) and 2 (blue). The scenarios are defined in the main text. C_{sv} changes with incrementally increased meltwater for these two scenarios. C_{sv} sediment particle density = 2650 $kg\ m^{-3}$. Points A^{1-3} and C^{1-4} are defined in Tables 2 and 3. B^{1-4} intersect with the two curves.

Table 4
Average suspended particle concentrations values (C_{sav}) calculated from mixing estimated sediment volumes for three scenarios with meltwater volumes derived from Equation (1).

	Volume of sediment (km^3)	Volume of freshwater (km^3)	Equivalent global sea-level rise (m)	C_{sav} (kg m^{-3})
Scenario 1	1000	88806 ($C^{2,3}$)	0.246	29.84 (A^2)
Scenario 2	133	88806 ($C^{2,3}$)	0.246	3.98 (A^3)
Scenario 3	1000 + 3500 (Storegga)	88806	0.246	134.28

The points denoted in Fig. 7 are indicated with brackets.

considerably higher during times of peak discharge (i.e., the short duration seasonal melt).

Scenario 3, with the Storegga slide volume added to the volume of laminated sediments in the Nordic Seas, provides an estimate of the maximum average suspended particle concentration. To achieve a critical suspended particle concentration of 43.5 kg m^{-3}, a freshwater volume of nearly 274000 km^3 would be needed (Table 3), which far exceeds the available meltwater volume (V_{MW}) derived from the $\delta^{18}O_{npl}$ of ∼89000 km^3. When the sediment volume for scenario 3 (4500 km^3) is mixed with V_{MW}, a C_{sav} of 134 kg m^{-3} is obtained (Table 4). For scenario 3, meltwater would be injected hyperpycnally into the Nordic Seas. Considering all three scenarios, we conclude that the laminated Nordic Seas sediments deposited during H1 likely represent hyperpycnites, originating from Scandinavian ice sheet melt.

At ∼15.5 ka BP, intense northern high-latitude cooling (Alm, 1993; Fig. 5f) caused re-advance of the Scandinavian ice sheet (Rinterknecht et al., 2006). $\delta^{18}O$ records from the Nordic Seas and Eirik Drift returned to heavier values, and finely laminated silt and clay were no longer deposited in the Nordic Seas. The gradual returns to heavier $\delta^{18}O_{npl}$ in the Nordic Seas and at Eirik Drift indicate that freshened waters were being purged out of the Nordic Seas, possibly due to wind-driven circulation and/or to a density gradient between the Nordic Seas and North Atlantic (e.g., Millo et al., 2006). Only a few centuries after the meltwater purging began to decrease, the AMOC recovered sharply at the time of and possibly causing (McManus et al., 2004) the abrupt Bølling warming (Fig. 4f, g).

4.4. A new conceptual model for the Nordic Seas and northern North Atlantic during H1

We propose a new concept for the sequence of events associated with the H1 iceberg/meltwater perturbation in the North Atlantic. We discuss a succession of three phases during H1 from both the marine and terrestrial realms. Phase 1 (∼19–17.5 ka BP) represents the onset of AMOC collapse, while phase 2 (17.5–16.7 ka BP) spans the main H1 phase in the IRD belt. Phase 2 is defined as the 'conventional' Heinrich event *sensu stricto* (HE-ss) and represents the intense IRD deposition and freshening event in the IRD belt, at the time of the "Heinrich layers" (Heinrich, 1988; Bond et al., 1992, 1999; Bond and Lotti, 1995; Grousset et al., 2000, 2001; Scourse et al., 2000; Hemming et al., 2000, 2002; Knutz et al., 2001, 2007; Hemming and Hajdas, 2003; Hemming, 2004). Phase 3 (16.7–14.6 ka BP) covers H1 in the Nordic Seas and at Eirik Drift and the termination of H1 cooling and AMOC resumption at the Bølling warm transition. Contrary to previous suggestions (e.g., Dowdeswell et al., 1995; Elliot et al., 1998; Rohling et al., 2003; Hemming, 2004; Roche et al., 2004), the entire sequence of paleoceanographic changes associated with H1, as proposed here, extends over almost 4000 years. We call this longer duration for the Heinrich event sequence, which includes all three phases, Heinrich event *sensu lato* (HE-sl). HE-sl spans the entire period of collapsed Nordic Seas deep-water formation, from onset to weakening, nearly complete collapse, through to sharp resumption at the Bølling warming (McManus et al., 2004; Stanford et al., 2006).

4.4.1. Phase 1: onset of AMOC collapse (∼19–17.5 ka BP)

From ∼26 to 21 ka BP, most circum-North Atlantic ice sheets had reached their maximum (LGM) extents, as indicated by sea-level records (e.g., Fairbanks, 1989; Bard et al., 1990a, b; Hanebuth et al., 2000, 2009; Yokoyama et al., 2000; Lambeck et al., 2002; Peltier and Fairbanks, 2006). From ∼21 ka BP, warming is inferred from Scandinavian pollen records (Alm, 1993) and Greenland ice core $\delta^{18}O$ (Andersen et al., 2006; Rasmussen et al., 2006, 2008; Svensson et al., 2006), as also noted by Bauch et al. (2001). The AMOC gradually slowed from ∼19 ka BP, culminating in a collapse from ∼17.5 ka BP (McManus et al., 2004; Hall et al., 2006; Stanford et al., 2006; Fig. 4g), which coincided with the onset of HE-ss1 in the IRD belt (e.g., Bond et al., 1992, 1999; Bard et al., 2000; Grousset et al., 2001; Hemming, 2004; Fig. 4c–e). The AMOC slowdown clearly predates the start of H1, as identified by peak IRD in the IRD belt, by more than 1000 years. Consequently, the widespread ice rafting cannot be invoked as the root cause of AMOC weakening from ∼19 ka BP. Instead, precursory freshwater events are a more likely mechanism for the AMOC slowdown.

Precursor IRD events have been identified in North Atlantic cores from the IRD belt, up to 1500 yrs prior to the main ice rafting; provenance studies indicate significant contributions of sediment derived from the European, Icelandic and Scandinavian ice sheets (e.g., Bond et al., 1992, 1997; 1999; Bond and Lotti, 1995; Darby and Bischof and Darby, 1999; Grousset et al., 2000, 2001; Scourse et al., 2000; Knutz et al., 2001; Hemming et al., 2000, 2002; Hemming and Hajdas, 2003; Hemming, 2004; Jullien et al., 2006; Peck et al., 2006, 2007a, b, 2007; Walden et al., 2007). A (partly) European/Scandinavian origin has been validated by the contemporaneous increase in fluvial input to the northern Bay of Biscay (Menot et al., 2006). This has led to the suggestion that early surging from European ice sheets may have stimulated a reaction from the Laurentide ice sheet (e.g., Grousset et al., 2000, 2001), which was the 'key player' in the main Heinrich events (e.g., Marshall and Koutnik, 2006). Precursor IRD-rich layers have also been identified in the Arctic, with a possible source from the Canadian Arctic Archipelago (Darby et al., 1997, 2002; Stokes et al., 2005). This timing for the onset of northern high-latitude warming (∼19 ka BP) coincides with the start of a warming trend in the EPICA Dronning Maud Land (EDML) ice core (EPICA Community Members, 2006), and increased northern summer insolation (Berger, 1991). This warming due to insolation, and changes in greenhouse gas and albedo feedbacks (e.g., Bender et al., 1997; Alley and Clark, 1999) may have promoted reduction of the relatively 'small' European and Scandinavian ice sheets (e.g., Stocker and Wright, 1991; McCabe and Clark, 1998; Stocker, 2003). Warming may also have been promoted due to Southern Ocean meltwater perturbations that enhanced AMOC intensity (Knorr and Lohmann, 2007), or alternatively, due to increased heat flow between the Indian and Atlantic Oceans via enhanced 'Agulhas leakage' (Peeters et al., 2004). We suggest that warming-induced northern hemisphere meltwater perturbations at ∼19 ka BP reduced the AMOC intensity

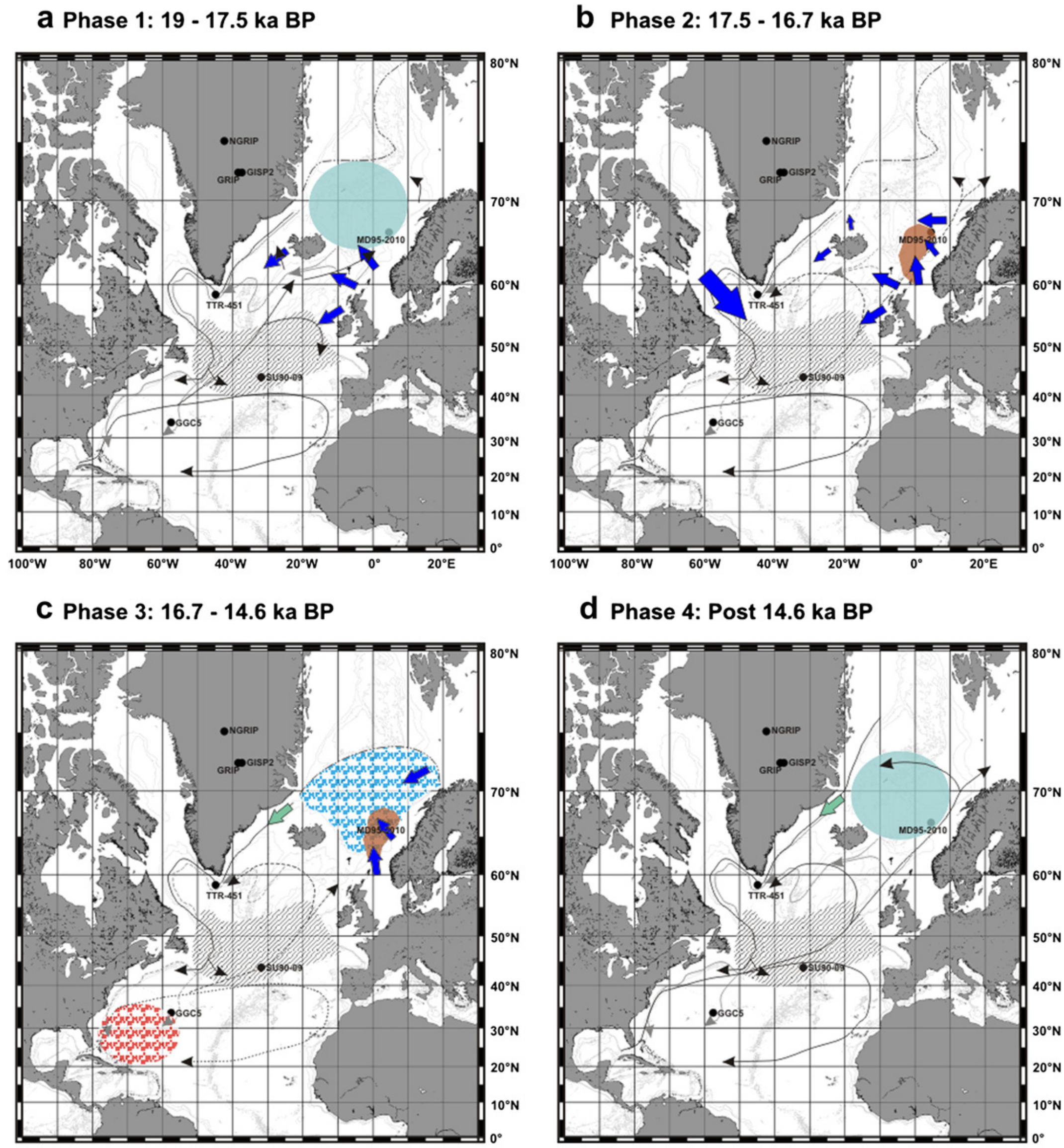

Fig. 8. Schematic diagrams of the evolution of H1 in the Nordic Seas and North Atlantic. Black lines indicate surface water currents, and dashed black lines indicate possible reduced flow intensity of thermohaline surface currents. Solid grey lines represent bottom currents and dashed grey lines indicate when bottom current flow intensity was significantly decreased. In Fig. 8a, the surface currents are after Pflaumann et al. (2003). Solid blue arrows = inferred ice sheet surges. Note, we also include the inferred freshening from the Barents ice sheet and from the northwestern Icelandic ice sheet after Sarnthein et al. (2001). Solid green arrow = Nordic Seas/Eirik Drift surface water mass communication (as inferred from this study). Light blue shaded zone = sites of NADW formation. Hashed black zone = IRD belt (after Hemming, 2004). Dot/dashed line represents the summer sea-ice margin. Blue hashed area = subsurface freshening in the Nordic Seas. Brown shaded area = high rates of sediment accumulation (Lekens et al., 2005). Orange hashed area represents inferred increased surface water salinity (Schmidt et al., 2004).

(similar to suggestions by Ganopolski and Rahmstorf, 2001). In response to northern cooling associated with AMOC slowdown (Fig. 4g), a short re-advance of the British and southern Laurentide ice-sheets occurred from ~18.2 ka BP (Bowen et al., 2002; Dyke et al., 2002; Fig. 5f).

4.4.2. *Phase 2: 'main' HE-ss1 phase (17.5–16.7 ka BP)*

The main HE-ss1 phase (~17.5–~16.7 ka BP) was characterised by maximum freshening and intense IRD deposition in the IRD belt, with consequently reduced numbers of foraminifera (Bond et al., 1992, 1999; Bond and Lotti, 1995; Grousset et al., 2000, 2001; Scourse et al., 2000; Hemming et al., 2000, 2002; Knutz et al., 2001, 2007; Hemming and Hajdas, 2003; Hemming, 2004; Peck et al., 2006, 2008; Fig. 4c–e) and a sustained AMOC collapse from ~17.5 ka BP (e.g., McManus et al., 2004; Hall et al., 2006; Stanford et al., 2006, Fig. 4g). Sarnthein et al. (2007) suggest that at around this time, an estuarine like reverse flow initiated over the Denmark Strait, evidenced by a pronounced increase in benthic foraminiferal ventilation ages in the Icelandic Sea, which were also younger than the ventilation ages of surface waters recorded in the planktonic foraminifera at the same core site. However, the mechanism by which inflowing, old intermediate waters may have overcome the steep topographic gradient of the (relatively shallow) Denmark Strait is problematic. From around 17.5 ka BP, cooling is indicated in Britain (Atkinson et al., 1987), Scandinavia (Alm, 1993), and the North Atlantic (Bard et al., 2000), as well as in Greenland, along with a sharp increase in ice core Ca^{2+} ion concentration, which indicates enhanced polar atmospheric circulation and/or a reorganisation of circulation patterns (Biscaye et al., 1997; Mayewski et al., 1997; Rohling et al., 2003; Andersen et al., 2006; Svensson et al., 2006; Jullien et al., 2006; Rasmussen et al., 2008).

Coeval with the onset of the main H1 phase, at ~17.5 ka BP, widespread and significant glacial retreats occurred on a nearly global scale (e.g., Giraudi and Frezzotti, 1997; Denton et al., 1999; Dyke et al., 2002 and references therein; Bowen et al., 2002; Clague and James, 2002; Licciardi et al., 2004; Ivy-Ochs et al., 2006; Menot et al., 2006; Rinterknecht et al., 2006), and a drawdown of the ice centre around the Hudson Bay region led to reorganisation of northeastern Laurentide ice-streams (Dyke et al., 2002; Fig. 8b). Significantly increased sedimentation rates indicate that large volumes of freshwater were delivered into the Nordic Seas at this time (Hjelstuen et al., 2004; Sejrup et al., 2004; Lekens et al., 2005). We re-interpret these deposits as hyperpycnites, which formed due to settling from deep sediment-laden meltwater injections (Fig. 8b). Note also that freshwater dilution has been documented in sediment cores that would have been located in front of the Barents ice shelf (Sarnthein et al., 2001). Following previous work (e.g., Broecker, 1991, 1994; 2000; Rahmstorf, 1994; Manabe and Stouffer, 2000; Ganopolski and Rahmstorf, 2001; McManus et al., 2004; Rahmstorf et al., 2005), we suggest that significant freshwater perturbations associated with iceberg discharges into the North Atlantic (as inferred from light planktonic $\delta^{18}O$ isotope values and thick IRD layers in the IRD belt) (e.g., Hemming, 2004, Fig. 4d,e) likely kept the AMOC in a collapsed state (Fig. 4g), which caused significantly reduced northern hemisphere temperatures and possible changed patterns of northern hemisphere seasonality (Fig. 5a, g).

4.4.3. Phase 3: H1 ‘clean-up’ and AMOC resumption (16.7–14.6 ka BP)

The final phase of H1 started at 16.7 ka BP with rapid reduction in surface-water freshening and IRD deposition in the IRD belt (Fig. 5c, d, 8). However, sustained cooling is apparent in Greenland ice core $\delta^{18}O$ records (Fig. 5a), and in Britain and Scandinavia (Fig. 5f), while Greenland Ca^{2+} ions suggest that atmospheric polar circulation remained relatively intense (Fig. 5c). The AMOC remained collapsed (Fig. 4g). The British ice sheet and Apennine glaciers re-advanced at around this time (Giraudi and Frezzotti, 1997; McCabe and Clark, 1998; McCabe et al., 2007). Unlike the decreased freshening inferred from IRD and $\delta^{18}O_{npl}$ records from the IRD belt, there are no signs of decreased surface water freshening at Eirik Drift or in the Nordic Seas (Fig. 4e, f). On the contrary, surface water freshening in both benthic and planktonic records started to increase at ~16.7 ka BP (Fig. 4e, f). Given the low IRD flux at Eirik Drift (i.e., freshwater had a non-iceberg source (Fig. 4d)) and that $\delta^{18}O_{npl}$ records have the same absolute values and variability as those of the Nordic Seas (Fig. 4f), we suggest that there was direct surface water communication between the Nordic Seas and Eirik Drift during this latter phase of H1.

Maximum surface freshening at Eirik Drift is suggested at ~15.1 ka BP (Fig. 4f). Thereafter, surface $\delta^{18}O_{npl}$ progressively returned to heavier values, coincident with re-advance of the Scandinavian ice sheet (Marks, 2002; Rinterknecht et al., 2006; Fig. 5f) and termination of exceptionally rapid deposition of fine-grained sediments in the Nordic Seas (Lekens et al., 2005; bright green line in Fig. 5f). Above, we interpreted these fine-grained sediments as hyperpycnal flows that injected significant freshwater into intermediate depths of the Nordic Seas, followed by transfer (mixing) of the light $\delta^{18}O$ signal from intermediate depths to the surface. As the AMOC was collapsed during the main phase of H1 (Fig. 4g), these relatively freshwaters would have ‘pooled’ in the Nordic Seas, which may explain why the AMOC remained in its collapsed state (Fig. 4g) despite the fact that iceberg-produced freshwater forcing in the open North Atlantic had ceased already (Fig. 4d and e). Mass balance dictates that these freshened Nordic Seas waters would have been expelled at the surface, notably through Denmark Strait, given that the Bering Strait was closed and that no deep waters exited from the Nordic Seas (Fig. 4g). Hence, $\delta^{18}O_{npl}$ signals at Eirik Drift appear to record the largely iceberg-free meltwater admixture as it was purged from the Nordic Seas. Heavier $\delta^{18}O$ after 15.1 ka BP suggests reduced freshwater admixture in the Nordic Seas, due to reduced meltwater input into the basin.

From ~15.5 ka BP, significant climate amelioration is recorded in the British Isles (Atkinson et al., 1987) and accelerating retreat from the H1 glacial maximum extent was well underway on a nearly global scale (Giraudi and Frezzotti, 1997; Benson et al., 1998; McCabe and Clark, 1998; Clague and James, 2002; Dyke et al., 2002 and references therein; Ivy-Ochs et al., 2006; McCabe et al., 2007; Hendy and Cosma, 2008). However, no warming occurred at northern high-latitudes (Alm, 1993; Rasmussen et al., 2006, 2008) or in well-dated lower latitude records (e.g., Hughen et al., 1996; von Grafenstein et al., 1999; Wang et al., 2001; Lea et al., 2003), which show excellent signal comparison with ice core $\delta^{18}O$ changes in Greenland (Rasmussen et al., 2006; Rohling et al., 2009), until the sharp Bølling (~15 °C) warming at 14.6 ka BP (Severinghaus and Brook, 1999; Rasmussen et al., 2006). Denton et al. (2005) suggested that records with close similarity to Greenland $\delta^{18}O$ may be biased toward winter conditions, and speculated that improving summer conditions caused the apparent ‘mismatch’ with datings of snowline variations. Denton et al. (2005) also suggested that increased winter sea-ice cover at northern high latitudes may have caused increased seasonality, consonant with suggestions by Broecker (2001) and Seager and Battisti (2007).

Model investigations suggest that Southern Ocean perturbations may have caused the AMOC ‘switch on’ at the Bølling warming (e.g., Weaver et al., 2003; Knorr and Lohmann, 2003). Ocean-circulation model results indicate that low latitude North Atlantic salt retention during AMOC collapse may have preconditioned the AMOC to kick start at the Bølling warming by advecting more saline surface waters to areas of NADW formation (Knorr and Lohmann, 2007). This model outcome agrees with sea surface salinity estimates for the Caribbean during the final H1 phase (Schmidt et al., 2004) and with Mediterranean salinity input (Rogerson et al., 2004). Liu et al. (2009) use an ocean-climate model to suggest that a complete cessation of freshwater forcing alone may have switched the AMOC back on at the Bølling warming. However, such a complete cessation of North Atlantic freshening is not validated by the paleo-data (Fig. 5d, e).

We suggest that after 15.1 ka BP, termination of freshwater injection from the Scandinavian ice sheet into the Norwegian Sea (Lekens et al., 2005), and purging of accumulated freshwater out of the Nordic Seas, would have (additionally) allowed gradually increased salinity. A few centuries after the freshwater purging flux began to decrease, the AMOC recovered sharply (McManus et al., 2004; Stanford et al., 2006; Fig. 4g) at the abrupt Bølling warming (14.6 ka BP) (Fig. 4a). We therefore suggest that increasing the salinity of the Nordic Seas prepared this key region of NADW formation (e.g., Dickson and Brown, 1994; Bacon, 1998, 2002) for the sharp AMOC recovery (Fig. 8d).

5. Conclusions

We identify four key oceanographic changes during HE-sl1, namely: (1) from 19–17.5 ka BP, a slowdown of NADW formation and small-scale precursor, iceberg-produced, meltwater events; (2) between 17.5 and 16.7 ka BP, a large-scale iceberg release and melting in the open North Atlantic IRD belt and a near shutdown of Nordic Seas deep-water formation (HE-ss1); (3) pooling of hyperpycnally injected freshwater in the Nordic Seas, and sustained AMOC collapse between 16.7 and 15.1 ka BP, and (4) after 15.1 ka BP, a subsequent purging of pooled meltwater out of the Nordic Seas. Termination of this final meltwater 'clean-up' phase was nearly coincident with the AMOC recovery that accompanied Bølling warming. The entire sequence of events extends the duration of the 'wider Heinrich event 1 sequence' (HE-sl1) to almost 4000 years, rather than to several centuries as previously suggested (e.g., Dowdeswell et al., 1995; Elliot et al., 1998; Rohling et al., 2003; Hemming, 2004; Roche et al., 2004), which only represent HE-ss1. This longer total duration of the H1 episode (HE-sl1) now agrees with the entire previously established period of collapsed Nordic Seas deep-water formation (McManus et al., 2004; Stanford et al., 2006).

Acknowledgements

This study was supported by the Natural Environment Research Council as part of the RAPID (NER/T/S/2002/00453), QUEST deglaciation (NE/D001773/1) and RESET (NE/E01531X/1) programmes. We acknowledge the crew and scientists onboard *R/V ProfessorLogachev* and BOSCORF. We also thank Leibniz Labor, Kiel, for the AMS ^{14}C datings, S.E. Hunter for assistance with measurements from core TTR-451, and D.A.V. Stow and S.O. Rasmussen for insightful comments and suggestions.

Appendix. Supplementary data

Supplementary data associated with this article can be found in the on-line version, at doi:10.1016/j.quascirev.2011.02.003.

References

Aagaard, K., Carmack, E.C., 1989. The role of sea ice and other fresh water in the Arctic Circulation. Journal of Geophysical Research 94, 14485–14498.

Alley, R.B., Clark, P.U., 1999. The deglaciation of the Northern hemisphere: a global perspective. Annual Reviews of Earth and Planetary Sciences 27, 149–182.

Alm, T., 1993. Øvre Æråsvatn – palynostratigraphy of a 22,000 to 10,000 BP lacustrine record on Andøya, northern Norway. Boreas 22, 171–188.

Andersen, K.K., Svensson, A., Johnsen, S.J., Rasmussen, S.O., Bigler, M., Röthlisberger, R., Ruth, U., Siggaard-Andersen, M.-L., Steffensen, J.P., Dahl-Jensen, D., Vinther, B.M., Clausen, H.B., 2006. The Greenland ice core chronology 2005, 15–42 ka. Part 1: constructing the time scale. Quaternary Science Reviews 25, 3246–3257.

Arz, H.W., Patzold, J., Wefer, G., 1999. The deglacial history of the western tropical Atlantic as inferred from high resolution stable isotope records off northeastern Brazil. Earth and Planetary Science Letters 167, 105–117.

Atkinson, T.C., Briffa, K.R., Coope, G.R., 1987. Seasonal temperatures in Britain during the past 22,000 years, reconstructed using beetle remains. Nature 325, 587–592.

Bacon, S., 1998. Decadal variability in the outflow from the Nordic seas to the deep Atlantic Ocean. Nature 394, 871–874.

Bacon, S., 2002. The dense overflows from the Nordic seas into the deep north Atlantic. ICES Marine Science Symposia 215, 148–155.

Bacon, S., Reverdin, G., Rigor, I.G., Snaith, H.M., 2002. A freshwater jet on the East Greenland Shelf. Journal of Geophysical Research 107 (C7), 3068,. doi:10.1029/2001JC000935.

Banerjee, S.K., King, J.W., Marvin, J., 1981. A rapid method for magnetic granulometry with applications to environmental studies. Geophysical Research Letters 8, 333–336.

Bard, E., Hamelin, B., Fairbanks, R.G., Zindler, A., 1990a. Calibration of the ^{14}C timescale over the past 30,000 years using mass spectrometric U–Th ages from Barbados corals. Nature 345, 405–410.

Bard, E., Hamelin, B., Fairbanks, R.G., 1990b. U/Th ages obtained by mass spectrometry in corals from Barbados – sea level during the past 130,000 years. Nature 346, 456–458.

Bard, E., Arnold, M., Mangerud, J., Paterne, M., Labeyrie, L., Duprat, J., Mélières, M.-A., Sønstegaard, E., Duplessy, J.-C., 1994. The North Atlantic atmosphere-sea surface ^{14}C gradient during the Younger Dryas climatic event. Earth and Planetary Science Letters 126, 275–287.

Bard, E., Rostek, F., Turon, J.-L., Sonzogni, C., 2000. Interhemispheric synchrony of the last deglaciation inferred from alkenone paleothermometry. Nature 385, 707–710.

Bauch, H.A., Erlenkeuser, H., Spielhagen, R.F., Struck, U., Matthiessen, J., Thiede, J., Heinemeier, J., 2001. A multiproxy reconstruction of the evolution of deep and surface waters in the subarctic Nordic seas over the last 30,000 yr. Quaternary Science Reviews 20, 659–678.

Bauch, D., Bauch, H., 2001. Last glacial benthic foraminiferal $\delta^{18}O$ anomalies in the polar North Atlantic: a modern analogue evaluation. Journal of Geophysical Research 106 (C5), 9135–9143.

Bender, M., Sowers, T., Brook, E., 1997. Gases in ice cores. Proceedings of the National Academy of Science 94, 8343–8349.

Benetti, S., 2006, Late Quaternary sedimentary processes along the western North Atlantic margin, Ph.D. Thesis, 188 pp., Univ. of Southampton, Southampton, UK.

Benson, L.V., May, H.M., Antweiler, R.C., Brinton, T.I., Kashgarian, M., Smoot, J.P., Lund, S.P., 1998. Continuous lake-sediment records of glaciation in the Sierra Nevada between 52,600 and 12,500 ^{14}C yr B.P. Quaternary Research 50, 113–127.

Berger, A., 1991. Insolation values for the climate of the last 10 million of years. Quaternary Science Reviews 10, 297–317.

Berger, A., 1999. Parameters of the Earths orbit for the last 5 Million years in 1 kyr resolution. PANGAEA, doi:10.1594/PANGAEA.56040.

Bigler, M., 2004. Hochauflösende Spurenstoffmessungen an polaren Eisbohrkernen: Glaziochemische und klimatische Prozessstudien. Ph.D. dissertation, University of Bern, Switzerland.

Biscaye, P.E., Grousset, F.E., Revel, M., Vander Gaast, S., Zielinski, G.A., Vaars, A., Kukla, G., 1997. Asian provenance of glacial dust (stage 2) in the Greenland Ice Sheet Project 2 ice core, Summit, Greenland. Journal of Geophysical Research 102 (C12), 26765–26781.

Bischof, J.F., Darby, D.A., 1999. Quaternary ice transport in the Canadian Arctic and extent of late Wisconsinan glaciation in the Queen Elizabeth Islands. Canadian Journal of Earth Sciences 36, 2007–2022.

Bond, G.W., Heinrich, H., Broecker, W., Labeyrie, L., McManus, J., Andrews, J., Huon, S., Jantschik, R., Clasen, S., Simet, C., Tedesco, K., Klas, M., Bonani, G., Ivy, S., 1992. Evidence for massive discharges of icebergs into the North Atlantic Ocean during the last glacial period. Nature 360, 245–249.

Bond, G.C., Lotti, R., 1995. Iceberg discharges into the North Atlantic on millennial time scales during the Last Glaciation. Science 267, 1005–1009.

Bond, G., Showers, W., Cheseby, M., Lotti, R., Almasi, P., deMenocal, P., Priore, P., Cullen, H., Hajdas, I., Bonani, G., 1997. A pervasive millennial-scale cycle in North Atlantic Holocene and glacial climates. Science 278, 1257–1266.

Bond, G., Showers, W., Elliot, M., Evans, M., Lotti, R., Hajdas, I., Bonani, G., Johnson, S., 1999. The north Atlantic's 1–2 kyr climate rhythm: relation to Heinrich events, Dansgaard/Oeschger cycles and the little ice age. In: Clark, P.U., Webb, R.S., Keigwin, L.D. (Eds.), Mechanisms of Global Climate Change at Millennial Time Scales. American Geophysical Union, Washington, D.C, pp. 35–58.

Bondevik, S., Svendsen, J.I., Johnsen, G., Mangerud, J., Kaland, P.E., 1997. The Storegga tsunami along the Norwegian coast, its age and runup. Boreas 26, 29–53.

Bondevik, S.J., Mangerud, J., Dawson, S., Dawson, A., Lohne, Ø, 2003. Record-breaking height for 8000-year-old tsunami in the North Atlantic. Eos, Transactions, American Geophysical Union 84, 289–300.

Bondevik, S., Mangerud, J., Birks, H.H., Gulliksen, S., Reimer, P., 2006. Changes in north Atlantic radiocarbon reservoir ages during the Allerød and younger Dryas. Science 312, 1514–1517.

Bowen, D.Q., Phillips, F.M., McCabe, A.M., Knutz, P.C., Sykes, G.A., 2002. New data for the last glacial maximum in great Britain and Ireland. Quaternary Science Reviews 21, 89–101.

Boyle, E.A., Keigwin, L., 1987. North Atlantic thermohaline circulation during the past 20,000 years linked to high-latitude surface temperature. Nature 330, 35–40.

Boyle, E.A., 1992. Cadnium and $\delta^{13}C$ Paleochemical Ocean distributions during the stage 2 glacial maximum. Annual Reviews of Earth and Planetary Sciences 20, 245–287.

Broecker, W.S., 1991. The great ocean conveyor. Oceanography 4, 79–89.

Broecker, W.S., Bond, M., Klas, G., Clark, E., McManus, J., 1992. Origin of the northern Atlantic's Heinrich events. Climate Dynamics 6, 265–273.

Broecker, W.S., 1994. Massive iceberg discharges as triggers for global climate change. Nature 372, 421–424.

Broecker, W.S., 2000. Abrupt climate change: causal constraints provided by the paleoclimate record. Earth-Science Reviews 51, 137–154.

Bugge, T., Befring, S., Belderson, R.H., Eidvin, T., Jansen, E., Kenyon, N.H., Holtedahl, H., Sejrup, H.P., 1987. A giant three-stage submarine slide off Norway. Geo-Marine Letters 7, 191–198.

Broecker, W.S., 2001. The big climate amplifier ocean circulation-sea-ice-storminess-Dustiness-Albedo. In: Seidov, D., Haupt, B.J., Maslin, M. (Eds.), The Oceans and Rapid Climate Change: Past. Present, and Future. American Geophysical Union, Washington, D.C, pp. 53–56.

Chough, S.K., Hesse, R., 1985. Contourites from Eirik Ridge, south of Greenland. Sedimentary Geology 41, 185–199.

Clague, J.J., James, T.S., 2002. History and isostatic effects of the last ice sheet in southern British Columbia. Quaternary Science Reviews 21, 71–87.

Cortijo, E., Labeyrie, L., Vidal, L., Vautravers, M., Chapman, M., Duplessy, J.-C., Elliot, M., Arnold, M., Turon, J.-L., Auffret, G., 1997. Changes in sea surface hydrology associated with Heinrich event 4 in the North Atlantic Ocean between 40° and 60°N. Earth and Planetary Science Letters 146, 29–45.

Curry, W.B., Marchitto, T.M., McManus, J.F., Oppo, D.W., Laarkamp, K.L., 1999. Millennial-scale changes in ventilation of the thermocline, intermediate, and deep waters of the glacial North Atlantic. In: Clark, P.U., Webb, R.S., Keigwin, L.D. (Eds.), Mechanisms of Global Climate Change at Millennial Time Scales. American Geophysical Union, Washington, D.C, pp. 59–76.

Dahl-Jensen, D., Mosegaard, K., Gundestrup, N., Clow, G.D., Johnsen, S.J., Hansen, A.W., Balling, N., 1998. Past temperatures directly from the Greenland ice sheet. Science 282, 268–271.
Darby, D.A., Bischof, J.F., Jones, G.A., 1997. Radiocarbon chronology of depositional regimes in the western Arctic Ocean. Deep Sea Research, Part II 44, 1745–1757.
Darby, D.A., Bischof, J.F., Spielhagen, R.F., Marshall, S.A., Harman, S.W., 2002. Arctic ice export events and their potential impact on global climate during the late Pleistocene. Paleoceanography 17, 1025. doi:1029/2001PA000639.
de Vernal, A., Hillaire-Marcel, C., Peltier, W.R., Weaver, A.J., 2002. The structure of the upper water column in the northwest North Atlantic: modern vs. Last Glacial Maximum conditions. Paleoceanography 17 (4), 1050.
Denton, G.H., Heusser, C.J., Lowell, T.V., Moreno, P.I., Andersen, B.G., Heusser, L.E., Schülchter, C., Marchant, D.R., 1999. Interhemispheric linkage of paleoclimate during the last glaciation. Geografiska Annaler 81, 107–153.
Denton, G.H., Alley, R.B., Comer, G.C., Broecker, W.S., 2005. The role of seasonality in abrupt climate change. Quaternary Science Reviews 24, 1159–1182.
Dickson, R.R., Brown, J., 1994. The production of North Atlantic deep water: sources, rates and pathways. Journal of Geophysical Research 99, 12319–12341.
Dokken, T.M.J., Jansen, E., 1999. Rapid change in the mechanism of ocean convection during the last glacial period. Nature 401, 458–461.
Dowdeswell, J.A., Maslin, M.A., Andrews, J.T., McCave, I.N., 1995. Iceberg production, debris rafting, and the extent and thickness of Heinrich layers (H-1, H-2) in North Atlantic sediments. Geology 23, 301–304.
Duplessy, J.-C., Labeyrie, Julliet-Leclerc, L.A., Maitre, F., Duprat, J., Sarthein, M., 1991. Surface salinity reconstruction of the North Atlantic Ocean during the Last Glacial Maximum. Oceanologica Acta 14 (4), 311–324.
Dyke, A.S., Andrews, J.T., Clark, P.U., England, J.H., Miller, G.H., Shaw, J., Veillette, J.J., 2002. The Laurentide and Innuitian ice sheets during the last glacial maximum. Quaternary Science Reviews 21, 9–31.
Elliot, M., Labeyrie, L., Bond, G., Cortijo, E., Turon, J.-L., Tisnerat, N., Duplessy, J.-C., 1998. Millennial-scale iceberg discharges in the Irminger Basin during the last glacial period: relationship with Heinrich events and environmental settings. Paleoceanography 13, 433–446.
Elliot, M., Labeyrie, L., Duplessy, J.-C., 2002. Changes in North Atlantic deep-water formation associated with Dansgaard-Oeschger temperature oscillations (60–10 ka). Quaternary Science Reviews 21, 1153–1165.
EPICA Community Members, 2006. One-to-one coupling of glacial climate variability in Greenland and Antarctica. Nature 444, 195–198.
Fairbanks, R.G., 1989. A 17,000-year glacio-eustatic sea level record: influence of glacial melting rates on the Younger Dryas event and deep-ocean circulation. Nature 342, 637–642.
Fairbanks, R.G., Mortlock, R.A., Chiu, T.-C., Cao, L., Kaplan, A., Guilderson, T.P., Fairbanks, T.W., Bloom, A.L., Grootes, P.M., Nadeau, M.-J., 2005. Radiocarbon calibration curve spanning 0 to 50,000 years BP based on paired ^{230}Th/^{234}U/^{238}U and ^{14}C dates on pristine corals. Quaternary Science Reviews 24, 1781–1796.
Fohrmann, H., Backhaus, J.O., Blaume, F., Rumohr, J., 1998. Sediments in bottom-arrested gravity plumes: numerical case studies. Journal of Physical Oceanography 28, 2250–2274.
Fuhrer, K., Neftel, A., Anklin, M., Maggi, V., 1993. Continuous measurements of hydrogen peroxide, formaldehyde, calcium and ammonium concentrations along the new GRIP ice core from Summit, Central Greenland. Atmospheric Environment 27A, 1873–1880.
Ganopolski, A., Rahmstorf, S., Petoukhov, V., Claussen, M., 1998. Simulation of modern and glacial climates with a coupled global model of intermediate complexity. Nature 391, 351–356.
Ganopolski, A., Rahmstorf, S., 2001. Rapid changes of glacial climate simulated in a coupled climate model. Nature 409, 153–158.
Gasse, F., 2000. Hydrological changes in the African tropics since the Last Glacial Maximum. Quaternary Science Reviews 19, 189–211.
Gil, I.M., Keigwin, L.D., Abrantes, F.G., 2009. Deglacial diatom productivity and surface ocean properties over the Bermuda Rise, northeast Sargasso Sea. Paleoceanography 24, PA4101. doi:10.1029/2008PA001729.
Gildor, H., Tziperman, E., 2003. Sea-ice switches and abrupt climate change. In: Philosophical Transactions of the Royal Society A – Mathematical Physical and Engineering Sciences, vol. 361 1810, 1935–1942.
Giraudi, C., Frezzotti, M., 1997. Late Pleistocene glacial events in the central Apennines, Italy. Quaternary Research 48, 280–290.
Grousset, F.E., Labeyrie, L., Sinko, J.A., Cremer, M., Bond, G., Duprat, J., Cortijo, E., Huon, S., 1993. Patterns of ice rafted detritus in the glacial North Atlantic (40–55°N). Paleoceanography 8, 175–192.
Grousset, F.E., Pujol, C., Labeyrie, L., Auffret, G., Boelaert, A., 2000. Were the North Atlantic Heinrich events triggered by the behaviour of the European ice sheets? Geology 28, 123–126.
Grousset, F.E., Cortijo, E., Herve, L., Richter, T., Burdloff, D., Duprat, J., Weber, O., 2001. Zooming in on Heinrich layers. Paleoceanography 16, 240–259.
Hall, I.R., Moran, S.B., Zahn, R., Knutz, P.C., Shen, C.-C., Edwards, R.L., 2006. Accelerated drawdown of meridional overturning in the late-glacial Atlantic triggered by transient pre-H event freshwater perturbation. Geophysical Research Letters 33, L16616. doi:10.1029/2006GL026239.
Hanebuth, T., Stattegger, K., Grootes, P.M., 2000. Rapid flooding of the Sunda shelf: a late-glacial sea-level record. Science 288, 1033–1035.
Hanebuth, T., Stattegger, K., Bojanowski, A., 2009. Termination of the Last Glacial Maximum sea-level lowstand: the Sunda-Shelf data revisited. Global and Planetary Change 66, 76–84.
Hansen, L., 2004. Deltaic Infill of a deglaciated Arctic fjord, East Greenland: sedimentary facies and sequence stratigraphy. Journal of Sedimentary Research 74 (3), 422–437.
Heinrich, H., 1988. Origin and consequences of cyclic ice rafting in the Northeast Atlantic Ocean during the past 13,000 years. Quaternary Research 29, 142–152.
Hemming, S.R., Hajdas, I., 2003. Ice rafted detritus evidence from ^{40}Ar/^{39}Ar ages of individual hornblende grains for evolution of the southeastern Laurentide ice sheet since 43 ^{14}C ky. Quaternary International 99, 29–43.
Hemming, S.R., Bond, G.C., Broecker, W.S., Sharp, W.D., Klas-Mendelson, M., 2000. Evidence from ^{40}Ar/^{39}Ar ages of individual hornblende grains for varying Laurentide sources of iceberg discharges 22,000 to 10,500 yr B.P. Quaternary Research 54, 372–383.
Hemming, S.R., 2004. Heinrich events: massive Late Pleistocene detritus layers of the North Atlantic and their global imprint. Reviews of Geophysics 42, 1–43.
Hemming, S.R., Hall, C.M., Biscaye, P.E., Higgins, S.M., Bond, G.C., McManus, J.F., Barber, D.C., Andrews, J.T., Broecker, W.S., 2002. ^{40}Ar/^{39}Ar ages and ^{40}Ar* concentrations of fine-grained sediment fractions from North Atlantic Heinrich layers. Chemical Geology 182, 583–603.
Hendy, I.L., Cosma, T., 2008. Vulnerability of the Cordilleran ice sheet to iceberg calving during late Quaternary rapid climate change events. Paleoceanography 23, PA2101. doi:10.1029/2008PA001606.
Hesse, R., Khodabakhsh, S., 1998. Depositional facies of late Pleistocene Heinrich events in the Labrador sea. Geology 26, 103–106.
Hesse, R., Klauke, I., Ryan, W.B.F., Edwards, M.B., Piper, D.J.W., 1996. Imaging Laurentide ice sheet drainage into the deep sea: impact on sedimentation and bottom water. In: Geological Society of America Today, vol. 6 3–9.
Hesse, R., Rashid, H., Khodabakhsh, S., 2004. Fine-grained sediment lofting from meltwater-generated turbidity currents during Heinrich events. Geology 32, 449–452.
Hillaire-Marcel, C., Bilodeau, G., 2000. Instabilities in the Labrador Sea water mass structure during the last climatic cycle. Canadian Journal of Earth Science 37, 795–809.
Hillaire-Marcel, C., de Vernal, A., 2008. Stable isotopic clue to episodic sea ice formation in the glacial North Atlantic. Earth and Planetary Science Letters 268, 143–150.
Hjelstuen, B.O., Sejrup, H.P., Haflidason, H., Nygård, A., Berstad, I.M., Knorr, G., 2004. Late Quaternary seismic stratigraphy and geological development of the south Vøring margin, Norwegian Sea. Quaternary Science Reviews 23, 1847–1865.
Holliday, N.P., Bacon, S., Allen, J., McDonagh, E.L., 2009. Circulation and transport in the western boundary currents at Cape Farewell, Greenland. Journal of Physical Oceanography 39, 1854–1870.
Hughen, K.A., Overpeck, J.T., Peterson, L.C., Trumbore, S., 1996. Rapid climate changes in the tropical Atlantic region during the last deglaciation. Nature 380, 51–54.
Hunter, S.E., Wilkinson, D., Stanford, J.D., Stow, D.A.V., Bacon, S., Rohling, E.J., Akhetmetzhanov, A.M., Kenyon, N.H., 2007a. The Eirik drift: a long-term barometer of north Atlantic deepwater flux south of Cape Farewell, Greenland. In: Viana, A.R., Rebesco, M. (Eds.), Economic and Palaeoceanographic Significance of Contourite Deposits. Geological Society Special Publications, vol. 276, pp. 245–263.
Hunter, S.E., Wilkinson, D., Louarn, E., McCave, I.N., Rohling, E.J., Stow, D.A.V., Bacon, S., 2007b. Deep western boundary current dynamics and associated sedimentation on the Eirik Drift, Southern Greenland Margin. Deep-Sea Research I 54, 2036–2066.
Ivy-Ochs, S., Kerschener, H., Kubik, P.W., Schlüchter, C., 2006. Glacier response in the European Alps to Heinrich event 1 cooling: the Gschnitz stadial. Journal of Quaternary Science 21, 115–130.
Jullien, E., Grousset, F.E., Hemming, S.R., Peck, V.L., Hall, I.R., Jeantet, C., Billy, I., 2006. Contrasting conditions preceding MIS3 and MIS2 Heinrich events. Global and Planetary Change 54, 225–238.
Keigwin, L.D., Boyle, E.A., 2008. Did the North Atlantic overturning halt 17,000 years ago? Paleoceanography 23, PA1101. doi:10.1029/2007PA001500.
Kim, J.H., Schneider, R.R., Muller, P.J., Wefer, G., 2002. Interhemispheric comparison of deglacial sea-surface temperature patterns in Atlantic eastern boundary currents. Earth and Planetary Science Letters 203, 779–780.
Kissel, C., Laj, C., Labeyrie, L., Dokken, T., Voelker, A., Blamart, D., 1999. Magnetic signatures of rapid climatic variations in North Atlantic sediments. In: Mix, A. (Ed.), Reconstructing Ocean History: a Window into the Future. Kluwer Academic/Plenum Publishers, New York, pp. 419–437.
Kissel, C., Laj, C., Mulder, T., Wandres, C., Cremer, M., 2009. The magnetic fraction: a tracer of deep water circulation in the North Atlantic. Earth and Planetary Science Letters 288, 444–454.
Knorr, G., Lohmann, G., 2003. Southern ocean origin for the resumption of Atlantic thermohaline circulation during deglaciation. Nature 424, 532–536.
Knorr, G., Lohmann, G., 2007. Rapid transitions in the Atlantic thermohaline circulation triggered by global warming and meltwater during the last deglaciation. Geochemistry, Geophysics. Geosystems 8, Q12006. doi:10.1029/2007C001604.
Knutz, P.C., Austin, W.E.N., Jones, E.J.W., 2001. Millennial-scale depositional cycles related to British Ice Sheet variability and North Atlantic paleocirculation since 45 yr B. P., Barra Fan, U. K. margin. Paleoceanography 16, 53–64.
Knutz, P.C., Zahn, R., Hall, I.R., 2007. Centennial-scale variability of the British Ice Sheet: implications for climate forcing and Atlantic meridional overturning circulation during the last deglaciation. Paleoceanography 22, PA1207. doi:10.1029/2006PA001298.
Laj, C., Kissel, C., Mazaud, A., Michel, E., Muscheler, R., Beer, J., 2002. Geomagnetic field intensity, North Atlantic Deep Water circulation and atmospheric Δ^{14}C during the last 50 kyr. Earth and Planetary Science Letters 200, 177–190.

Lambeck, K., Yokoyama, Y., Purcell, T., 2002. Into and out of the Last Glacial Maximum: sea-level change during oxygen isotope stages 3 and 2. Quaternary Science Reviews 21, 343–360.
Lea, D.W., Pak, D.K., Peterson, L.C., Hughen, K.A., 2003. Synchroneity of tropical and high-latitude Atlantic temperatures over the last glacial termination. Science 301, 1361–1364.
Lekens, W.A.H., Sejrup, H.P., Haflidason, H., Petersen, G.Ø, Hjelstuen, B., Knorr, G., 2005. Laminated sediments preceding Heinrich event 1 in the Northern North Seas and Southern Norwegian Sea: origin, processes and regional linkage. Marine Geology 216, 27–50.
Licciardi, J.M., Clark, P.U., Brook, E.J., Elmore, D., Sharma, P., 2004. Variable responses of western U.S. glaciers during the last glaciation. Geology 32, 81–84.
Liu, Z., Otto-Bliesner, B.L., He, F., Brady, E.C., Tomas, R., Clark, P.U., Carlson, A.E., Lynch-Stieglitz, J., Curry, W., Brook, E., Erickson, D., Jacob, R., Kutzbach, J., Cheng, J., 2009. Transient simulation of last deglaciation with a new mechanism for the Bølling–Allerød warming. Science 325, 310–314.
MacAyeal, D.R., 1993. Binge/purge oscillations of the Laurentide ice sheet as a cause of the North Atlantic's Heinrich events. Paleoceanography 8, 775–784.
Manabe, S., Stouffer, R.J., 2000. Study of abrupt climate change by a coupled ocean-atmosphere model. Quaternary Science Reviews 19, 285–299.
Marks, L., 2002. Last glacial maximum in Poland. Quaternary Science Reviews 21, 103–110.
Marchitto, T.M., Lehman, S.J., Ortiz, J.D., Flückiger, J., van Geen, A., 2007. Marine radiocarbon evidence for the mechanism of deglacial atmospheric CO_2 rise. Science 316, 1456–1459.
Marshall, S.J., Koutnik, M.R., 2006. Ice sheet action versus reaction: distinguishing between Heinrich events and Dansgaard-Oeschger cycles in the North Atlantic. Paleoceanography 21, PA2021. doi:10.1029/2005PA001247.
Mayewski, P.A., Meeker, L.D., Whitlow, S., Twickler, M.S., Morrison, M.C., Bloomfield, P., Bond, G.C., Alley, R.B., Gow, A.J., Grootes, P.M., Meese, D.A., Ram, M., Taylor, K.C., Wumkes, W., 1994. Changes in atmospheric circulation and ocean ice cover over the North Atlantic during the last 41,000 years. Science 263, 1747–1751.
Mayewski, P.A., Meeker, L.D., Twickler, M.S., Whitlow, S., Yang, Q., Lyons, B., Prentice, M., 1997. Major features and forcing of high-latitude northern hemisphere atmospheric circulation using a 110,000-year-long glaciochemical series. Journal of Geophysical Research 102, 26345–26366.
McCabe, A.M., Clark, P.U., 1998. Ice-sheet variability around the North Atlantic Ocean during the last deglaciation. Nature 392, 373–376.
McCabe, A.M., Clark, P.U., Clark, J., 2005. AMS ^{14}C dating of deglacial events in the Irish Sea basin and other sectors of the British–Irish ice sheet. Quaternary Science Reviews 24, 1673–1690.
McCabe, A.M., Clark, P.U., Clark, J., Dunlop, P., 2007. Radiocarbon constraints on readvances of the British–Irish ice sheet in the northern Irish Sea basin during the last deglaciation. Quaternary Science Reviews 26, 1204–1211.
McManus, J.F., Francois, R., Gherardi, J.-M., Keigwin, L.D., Brown-Leger, S., 2004. Collapse and rapid resumption of Atlantic meridional circulation linked to deglacial climate changes. Nature 428, 834–837.
Meland, M.Y., Jansen, E., Elderfield, H., 2005. Constraints on SST estimates for the northern north Atlantic/Nordic seas during the LGM. Quaternary Science Reviews 24, 835–852.
Meland, M.Y., Dokken, T.M., Jansen, E., Hevrøy, K., 2008. Water mass properties and exchange between the Nordic seas and the northern North Atlantic during the period 23–6 ka: benthic oxygen isotopic evidence. Paleoceanography 23, PA1210. doi:10.1029/2007PA001416.
Menot, G., Bard, E., Rostek, R., Weijers, W.H., Hopmans, E.C., Schouten, S., Sinninghe Damsté, J.S., 2006. Early reactivation of European rivers during the last deglaciation. Science 313, 1623–1625.
Mignot, J., Ganopolski, A., Levermann, A., 2007. Atlantic subsurface temperatures: response to a shutdown of the overturning circulation and consequences for its recovery. Journal of Climate 20, 4884–4898.
Millo, C., Sarnthein, M., Voelker, A., Erlenkeuser, H., 2006. Variability of the Denmark overflow during the last glacial maximum. Boreas 35, 50–60.
Mix, A.E., Bard, E., Schneider, R., 2001. Environmental processes of the ice age: land, ocean, glaciers (EPILOG). Quaternary Science Reviews 20, 627–657.
Mulder, T., Syvitski, J.P.M., 1995. Turbidity currents generated at river mouths during exceptional discharges to the world oceans. Journal of Geology 103, 285–299.
Mulder, T., Migeon, S., Savoye, B., Faugères, J.-C., 2001. Inversely graded turbidite sequences in the deep Mediterranean. A record of deposits from flood-generated turbidity currents? Geo-Marine Letters 21, 86–93.
Mulder, T., Syvitski, J.P.M., Migeon, S., Faugéres, J.-C., Savoye, B., 2003. Marine hyperpycnal flows: initiation, behavior and related deposits. A review. Marine and Petroleum Geology 20, 861–882.
Nørgaard-Pederson, N., Spielhagen, R.F., Erlenkeuser, H., Grootes, P.M., Heinemeiner, J., Knies, J., 2003. Arctic Ocean during the Last Glacial Maximum: atlantic and polar domains of surface water mass distribution and ice cover. Paleoceanography 18, 1063. doi:10.1029/2002PA000781.
Nygård, A., Sejrup, H.P., Haflidason, H., Lekens, W.A.H., Clark, C.D., Bigg, G.R., 2007. Extreme sediment and ice discharge from marine-based ice streams: new evidence from the North Sea. Geology 35, 395–398.
Nygård, A., Sejrup, H.P., Haflidason, H., Lekens, W.A.H., Clark, Marcello, C., Ottesen, D., 2004. Deglaciation history of the southwestern Fennoscandian Ice Sheet between 15 and 13 ^{14}C ka BP. Boreas 33, 1–17.
Paul, A., Schulz, M., 2002. Holocene Climate Variability on Centennial-to-millennial Time Scales: 2. Internal and Forced Oscillations as Possible Causes. In: Wefer, G., Berger, W., Jansen, E. (Eds.), Climate Development and History of the North Atlantic Realm. Springer, Berlin, pp. 55–73.
Peck, V.L., Hall, I.R., Zahn, R., Elderfield, H., Grousset, F., Hemming, S.R., Scourse, J.D., 2006. High resolution evidence for linkages between NW European ice sheet instability and Atlantic meridional overturning circulation. Earth and Planetary Science Letters 243, 476–488.
Peck, V.L., Hall, I.R., Zahn, R., Grousset, F., Hemming, S.R., Scourse, J.D., 2007a. The relationship of Heinrich events and their European precursors over the past 60 ka BP: a multi-proxy ice-rafted debris provenance study in the North East Atlantic. Quaternary Science Reviews 26, 862–875.
Peck, V.L., Hall, I.R., Zahn, R., Scourse, J.D., 2007b. Progressive reduction in NE Atlantic ventilation prior to Heinrich events: response to NW European ice sheet instabilities? Geochemistry, Geophysics, Geosystems 8, Q01N10. doi:10.1029/2006GC001321.
Peck, V.L., Hall, I.R., Zahn, R., Elderfield, H., 2008. Millennial-scale surface and subsurface paleothermometry from the northeast Atlantic, 55–8 ka BP. Paleoceanography 23, PA3221. doi:10.1029/2008PA001631.
Peeters, F.J.C., Acheson, R., Brummer, G.J.A., de Ruijter, W., Schneider, R.R., Ganssen, G., Ufkes, E., Kroon, D., 2004. Vigorous exchange between the Indian and Atlantic oceans at the end of the past five glacial periods. Nature 430, 661–665.
Peltier, W.R., Fairbanks, R.G., 2006. Global ice volume and Last Glacial Maximum duration from an extended Barbados sea-level record. Quaternary Science Reviews 25, 3322–3337.
Pflaumann, U., Sarnthein, M., Chapman, M., d'Abreu, L., Funnell, B., Huels, M., Kiefer, T., Maslin, M., Schulz, H., Swallow, J., van Kreveld, S., Vautravers, M., Vogelsang, E., Weinelt, M., 2003. Glacial north Atlantic: sea-surface conditions reconstructed by GLAMAP 2000. Paleoceanography 18 (3), 1065. doi:10.1029/2002PA000774.
Rahmstorf, S., 1994. Rapid climate transitions in a coupled ocean-atmosphere model. Nature 372, 81–85.
Rahmstorf, S., 2002. Ocean circulation and climate over the past 120, 000 years. Nature 419, 207–214.
Rahmstorf, S., Crucifix, M., Ganopolski, A., Goose, H., Kamenkovich, I., Knutti, R., Lohmann, G., Marsh, R., Mysak, L.A., Wang, Z., Weaver, A.J., 2005. Thermohaline circulation hysteresis: a model intercomparison. Geophysical Research Letters 32, L23605. doi:10.1029/2005GL023655.
Rashid, H., Hesse, R., Piper, D.J.W., 2003. Distribution, thickness and origin of Heinrich layer 3 in the Labrador Sea. Earth and Planetary Science Letters 205, 281–293.
Rashid, H., Boyle, E.A., 2007. Mixed-layer deepening during Heinrich Events: a multi-planktonic foraminiferal $\delta^{18}O$ approach. Science 318, 439–441.
Rasmussen, S.O., Andersen, K.K., Svensson, A.M., Steffensen, J.P., Vinther, B.M., Clausen, H.B., Siggaard-Andersen, M.-L., Johnsen, S.J., Larsen, L.B., Dahl-Jensen, D., Bigler, M., Röthlisberger, R., Fischer, H., Goto-Azuma, K., Hansson, M.E., Ruth, U., 2006. A New Greenland Ice Core Chronology for the Last Glacial Termination. Journal of Geophysical Research 111, D06102. doi:10.1029/2005JD006079.
Rasmussen, S.O., Seierstad, I.K., Andersen, K.K., Bigler, M., Dahl-Jensen, D., Johnsen, S.J., 2008. Synchronization of the NGRIP, GRIP, and GISP2 ice cores across MIS 2 and palaeoclimatic implications. Quaternary Science Reviews 27, 18–28.
Rasmussen, T.L., Thomsen, E., Labeyrie, L., van Weering, T.C.E., 1996a. Circulation changes in the Faeroe – Shetland Channel correlating with cold events during the last glacial period (58–10 ka). Geology 24, 937–940.
Rasmussen, T.L., Thomsen, E., van Weering, T.C.E., Labeyrie, L., 1996b. Rapid changes in surface and deep water conditions at the Faeroe Margin during the last 58,000 years. Paleoceanography 11, 757–771.
Rasmussen, T.L., Bäckström, D., Heinemeier, J., Klitgaard-Kristensen, D., Knutz, P.C., Kuijpers, A., Lassen, S., Thomsen, E., Troelstra, S.R., van Weering, T.C.E., 2002a. The Faeroe–Shetland Gateway: late Quaternary water mass exchange between the Nordic seas and the northeastern Atlantic. Marine Geology 188, 165–192.
Rasmussen, T.L., Thomsen, E., Troelstra, S.R., Kuijpers, A., Prins, M.A., 2002b. Millennial-scale glacial variability versus Holocene stability: changes in planktic and benthic foraminifera faunas and ocean circulation in the North Atlantic during the last 60 000 years. Marine Micropaleontology 47, 143–176.
Rasmussen, T.L., Thomsen, E., 2004. The role of the North Atlantic Drift in the millennial timescale glacial climate fluctuations. Palaeoceanography, Palaeoecology, Palaeoclimatology 210, 101–116.
Rasmussen, T.L., Thomsen, E., 2008. Warm Atlantic water inflow to the Nordic seas 34–10 calibrated ka B.P. Paleoceanography 23, PA1201. doi:10.1029/2007PA001453.
Rasmussen, T.L., Thomsen, E., 2010. Stable isotope signals from brines in the Barents Sea: implications for brine formation during the last glaciation. Geology 37, 903–906.
Reimer, P.J., Baille, M.G.L., Bard, E., Bayliss, A., Beck, J.W., Blackwell, P.G., Bronk Ramsey, C., Buck, C.E., Burr, G.S., Edwards, R.L., Friedrich, M., Grootes, P.M., Guilderson, T.P., Hajdas, I., Heaton, T.J., Hogg, A.G., Hughen, K.A., Kaiser, K.F., Kromer, B., McCormac, G., Manning, S.W., Reimer, R.W., Richards, D.A., Southon, J.R., Talamo, S., Turney, C.S.M., van der Plicht, J., Weyhenmeyer, C.E., 2009. INTCAL09 and MARINE09 radiocarbon age calibration curves, 0–50,000 yrs Cal BP. Radiocarbon 51, 1111–1150.
Rinterknecht, V.R., Clark, P.U., Raisbeck, M., Yiou, F., Bitnas, A., Brook, E.J., Marks, L., Zelčs, V., Lunkka, J.-P., Pavlovskaya, I.E., Piotrowski, J.A., Raukas, A., 2006. The last deglaciation of the southeastern sector of the Scandinavian ice sheet. Science 311, 1449–1452.
Risebrobakken, B., Jansen, E., Andersson, C., Mjelde, E., Hevrøy, K., 2003. A high resolution study of Holocene paleoclimatic and paleoceanographic changes in the Nordic seas. Paleoceanography 18 (1), 1017. doi:10.1029/2002PA000764.

Robinson, L.F., Adkins, J.F., Keigwin, L.D., Southon, J., Fernandez, D.P., Wang, S.-L., Scheirer, D.S., 2005. Radiocarbon variability in the Western North Atlantic during the last deglaciation. Science 310, 1469–1473.
Roche, D., Paillard, D., Cortijo, E., 2004. Constraints on the duration and freshwater release of Heinrich event 4 through isotope modeling. Nature 432, 379–382.
Rogerson, M., Rohling, E.J., Weaver, P.P.E., Murray, J.W., 2004. The Azores front since the last glacial maximum. Earth and Planetary Science Letters 222, 779–789.
Rohling, E.J., Mayewski, P.A., Challenor, P., 2003. On the timing and mechanism of millennial-scale climate variability during the last glacial cycle. Climate Dynamics 20, 257–267.
Rohling, E.J., Liu, Q., Roberts, A.P., Stanford, J.D., Rasmussen, S.O., Langen, P.L., Siddall, M., 2009. Controls on the East Asian monsoon during the last glacial cycle, based on comparison between Hulu Cave and polar ice-core records. Quaternary Science Reviews 28, 3291–3302.
Sachs, J.P., Anderson, R.F., Lehman, S.J., 2001. Glacial surface temperatures of the southeast Atlantic Ocean. Science 293, 2077–2079.
Sarnthein, M., Winn, K., Jung, S., Duplessy, J.-C., Labeyrie, L., Erlenkeuser, H., Ganssen, G., 1994. Changes in east Atlantic deepwater circulation over the last 30,000 years: eight time slice reconstructions. Paleoceanography 9, 209–267.
Sarnthein, M., Stattegger, K., Dreger, D., Erlenkeuser, H., Grootes, P., Haupt, B., Jung, S., Kiefer, T., Kuhnt, W., Pflaumann, U., Schäfer-Neth, C., Schultz, H., Schultz, M., Seivdov, D., Simstisch, J., van Kreveld, S., Vogelsang, E., Völker, A., Weinelt, M., 2001. Fundamental modes and abrupt changes in North Atlantic circulation and climate over the last 60 ky – concepts, reconstructions and numerical modeling. In: Schäfer, P., Ritzrau, W., Schlüter, M., Thiede, J. (Eds.), The Northern North Atlantic. Springer, Berlin, pp. 365–410.
Sarnthein, M., Grootes, P.M., Kennett, J.P., Nadeau, M.-J., 2007. ^{14}C reservoir ages show deglacial changes in the ocean currents and carbon cycle. In: Schmittner, A., Chiang, J.C.H., Hemming, S.R. (Eds.), Ocean Circulation: Mechanisms and Impacts: Past and Future Changes in Meridional Overturning. Geophysical Monograph Series, 173, pp. 175–196.
Schmidt, M.W., Spero, H.J., Lea, D.W., 2004. Links between salinity variation in the Caribbean and North Atlantic thermohaline circulation. Nature 428, 160–163.
Schmittner, A., Saenko, O.A., Weaver, A.J., 2003. Coupling of the hemispheres in observations and simulations of glacial climate change. Quaternary Science Reviews 22, 659–671.
Scourse, J.D., Hall, I.R., McCave, I.N., Young, J.R., Sugdon, C., 2000. The origin of Heinrich layers: evidence from H2 for European precursor events. Earth and Planetary Science Letters 182, 87–195.
Seager, R., Battisti, D.S., 2007. Challenges to our understanding of the general circulation: abrupt climate change. In: Schneider, T., Sobel, A.H. (Eds.), The Global Circulation of the Atmosphere: Phenomena, Theory, Challenges. Princeton University Press, pp. 331–371.
Sejrup, H.P., Larsen, E., Landvik, J., King, E.L., Haflidason, H., Nesje, A., 2000. Quaternary glaciations in southern Fennoscandia: evidence from southwestern Norway and the northern North Sea region. Quaternary Science Reviews 19, 667–685.
Sejrup, H.P., Haflidason, H., Hjelstuen, B.O., Nygård, A., Bryn, P., Lien, R., 2004. Pleistocene development of the SE Nordic Seas margin. Marine Geology 213, 169–200.
Severinghaus, J.P., Sowers, T., Brook, E.J., Alley, R.B., Bender, M.L., 1998. Timing of abrupt climate change at the end of the Younger Dryas period from thermally fractionated gases in polar ice. Nature 391, 141–146.
Severinghaus, J.P., Brook, E., 1999. Abrupt climate change at the end of the last glacial period inferred from trapped air in polar ice. Science 286, 930–934.
Stanford, J.D., Rohling, E.J., Hunter, S.E., Roberts, A.P., Rasmussen, S.O., Bard, E., McManus, J., Fairbanks, R.G., 2006. Timing of mwp-1a and climate responses to meltwater injections. Paleoceanography 21, PA4103. doi:10.1029/2006PA001340.
Stanford, J. D., Hemingway, R., Rohling, E. J., Challenor, P. G., Medina-Elizalde, M., Lester, A. J., in press. Sea-level probabilities for the last deglaciation: a statistical analysis of far-field records. Global and Planetary Change.
Stocker, T.F., 2003. South dials north. Nature 424, 496–499.
Stocker, T.F., Wright, D.G., 1991. Rapid transitions of the ocean's deep circulation induced by changes in surface water fluxes. Nature 351, 729–732.
Stokes, C.R., Clark, C.D., Darby, D.A., Hodgson, D.A., 2005. Late Pleistocene ice export events into the Arctic Ocean form the M'Clure Strait ice stream, Canadian Arctic Archipelago. Global and Planetary Change 49, 139–162.
Stow, D.A.V., 1996. Deep seas. In: Reading, H.G. (Ed.), Sedimentary Environments: Processes, Facies and Stratigraphy. Blackwell Sciences, Oxford, pp. 395–453.
Stuiver, M., Grootes, P.M., 2000. GISP2 oxygen isotope ratios. Quaternary Research 53, 277–284.
Svensson, A., Andersen, K.K., Bigler, M., Clausen, H.B., Dahl-Jensen, D., Davies, S.M., Johnsen, S.J., Muscheler, R., Rasmussen, S.O., Röthlisberger, R., Steffensen, J.P., Vinther, B.M., 2006. The Greenland ice core chronology 2005, 15–42 ka. Part 2: comparison to other records. Quaternary Science Reviews 25, 23–24.
van Kreveld, S., Sarnthein, M., Erlenkeuser, H., Grootes, P., Jung, S., Nadeau, M.J., Pflaumann, U., Voelker, A., 2000. Potential links between surging ice sheets, circulation changes, and the Dansgaard-Oeschger cycles in the Irminger Sea, 60–18 kyr. Paleoceanography 15, 425–442.
Verosub, K.L., Roberts, A.P., 1995. Environmental magnetism: past, present, and future. Journal of Geophysical Research 100, 2175–2192.
Vidal, L., Labeyrie, L., van Weering, T.C.E., 1998. Benthic δ^{18}O records in the North Atlantic over the last glacial period (60–10 kyr): evidence for brine formation. Paleoceanography 13, 245–251.
Vidal, L., Schneider, R.R., Marchal, O., Bickert, T., Stocker, T.F., Wefer, G., 1999. Link between the North and South Atlantic during the Heinrich events of the last glacial period. Climate Dynamics 15, 909–919.
Vinther, B.M., Clausen, H.B., Johnsen, S.J., Rasmussen, S.O., Andersen, K.K., Buchardt, S.L., Seierstad, I.K., Siggaard-Andersen, M.-L., Steffensen, J.P., Svensson, A.M., 2006. A synchronized dating of three Greenland ice cores throughout the Holocene. Journal of Geophysical Research 111, D13102. doi:10.1029/2005JD006921.
von Grafenstein, U., Erlenkeuser, H., Brauer, A., Jouzel, J., Johnsen, S.J., 1999. A mid-European decadal isotope-climate record from 15,500 to 5000 years B.P. Science 284, 1654–1657.
Waelbroeck, C., Duplessy, J.-C., Michel, E., Labeyrie, L., Pallard, D., Duprat, J., 2001. The timing of the last deglaciation in North Atlantic climate records. Nature 412, 724–727.
Walden, J., Wadsworth, E., Austin, W.E.N., Peters, C., Scourse, J.D., Hall, I.R., 2007. Compositional variability of ice-rafted debris in Heinrich layers 1 and 2 on the northwest European continental slope identified by environmental magnetic analyses. Journal of Quaternary Science 22, 163–172.
Wang, Y.J., Cheng, H., Edwards, R.L., An, Z.S., Wu, J.Y., Shen, C.-C., Dorale, J.A., 2001. A high-resolution absolute-dated Late Pleistocene monsoon record from Hulu Cave, China. Science 294, 2345–2348.
Weaver, A.J., Marotzke, J., Cummins, P.F., Sarachik, E.S., 1993. Stability and variability of the thermohaline circulation. Journal of Physical Oceanography 23, 39–60.
Weaver, A.J., Saenko, O.A., Clark, P.U., Mitrovica, J.X., 2003. Meltwater pulse 1A from Antarctica as a trigger of the Bølling–Allerød warm interval. Science 299, 1709–1713.
Weinelt, M., Sarnthein, M., Pflaumann, U., Schulz, H., Jung, S., Erlenkeuser, H., 1996. Ice-free Nordic seas during the last glacial maximum? Potential sites of deepwater formation. Paleoclimates 1, 283–309.
Weinelt, M., Vogelsang, E., Kucera, M., Pflaumann, U., Sarnthein, M., Voelker, A., Erlenkeuser, H., Malmgren, B.A., 2003. Variability of North Atlantic heat transfer during MIS 2. Paleoceanography 18, 1071. doi:10.1029/2002PA000772.
Winton, M., 1997. The effect of cold climate upon North Atlantic Deep Water formation in a simple ocean-atmosphere model. Journal of Climate 39, 37–51.
Yokoyama, Y., Lambeck, K., Deckker, P.D., Johnston, P., Fifield, L.K., 2000. Timing of Last Glacial Maximum from observed sea level minima. Nature 406, 713–716.
Zaragosi, S., Eynaud, F., Pujol, C., Auffret, G.A., Turon, J.-L., Garlan, T., 2001. Initiation of the European deglaciation as recorded in the northwestern Bay of Biscay slope environments (Meriadzek Terrace and Trevelyan Escarpment): a multi-proxy approach. Earth and Planetary Science Letters 188, 493–507.